CTIPS

Center for Transformative Infrastructure Preservation and Sustainability

USDOT Region 8 University Transportation Center

CTIPS-26-006

P. Lu
Y. Huang
L. Xu
D. Zhang
Y. Mahmood

ASSESSING CONDITION OF REHABILITATED CONCRETE PAVEMENT WITH SLAB FRACTURING AND ASPHALT OVERLAY USING DISTRIBUTED FIBER OPTIC SENSORS

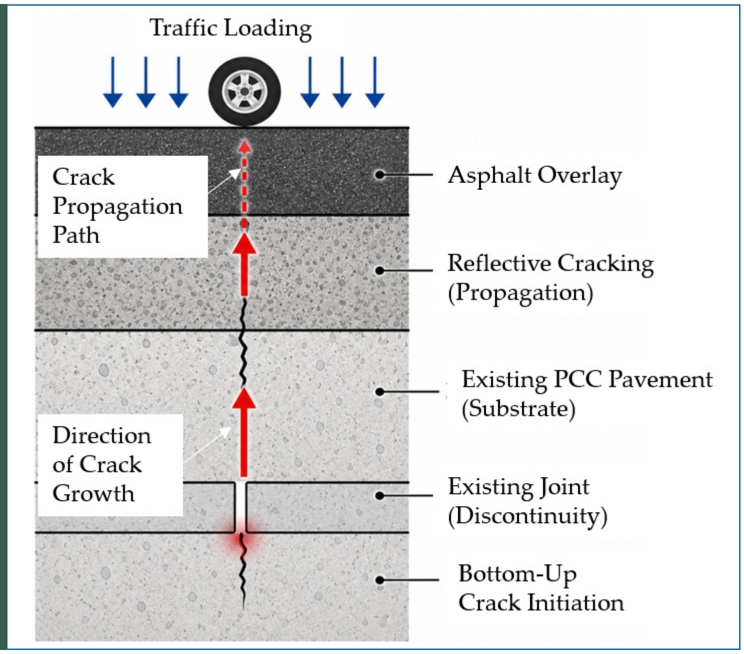

A University Transportation Center sponsored by the U.S. Department of Transportation serving the Center for Transformative Infrastructure Preservation and Sustainability members:

Colorado State University
Fort Lewis College
North Dakota State University
South Dakota State University
United Tribes Technical College
University of Colorado Denver
University of Denver
University of North Dakota
University of Utah
University of Wyoming
Utah State University

Technical Report Documentation Page

1. Report No.	2. Government Accession No.	3. Recipient's Catalog No.
CTIPS-26-006		

4. Title and Subtitle	5. Report Date
Assessing Condition of Rehabilitated Concrete Pavement with Slab Fracturing and Asphalt Overlay Using Distributed Fiber Optic Sensors	August 2026
	6. Performing Organization Code CTIPS
7. Author(s) ▪ Pan Lu https://orcid.org/0000-0002-1640-3598 ▪ Ying Huang https://orcid.org/0000-0003-4119-9522 ▪ Lyuang Xu https://orcid.org/0009-0000-3481-2080 ▪ Dawei Zhang https://orcid.org/0000-0002-0277-6342 ▪ Yasir Mahmood https://orcid.org/0009-0001-2887-2789	8. Performing Organization Report No. CTIPS-26-006
9. Performing Organization Name and Address Center for Transformative Infrastructure Preservation and Sustainability North Dakota State University PO Box 6050 Fargo, ND 58108	10. Work Unit No.
	11. Contract or Grant No. 69A3552348308
12. Sponsoring Agency Name and Address Department of Transportation Research and Innovative Technology Administration 400 7th Street, SW Washington, DC 20590	13. Type of Report and Period Covered Final Report
	14. Sponsoring Agency Code

15. Supplementary Notes

Conducted in cooperation with the U.S. Department of Transportation, Federal Highway Administration.

16. Abstract

Reflective cracking is one of the primary causes of premature deterioration in asphalt-overlaid Portland cement concrete (PCC) pavements, reducing service life and increasing maintenance costs. Because crack initiation begins within the underlying PCC layer before becoming visible at the surface, conventional inspection methods have limited capability for early detection. This project developed and experimentally validated a hybrid experimental-numerical framework that integrates optical frequency domain reflectometry (OFDR)-based distributed fiber optic sensing (DFOS), laboratory-scale three-point bending tests, and finite element (ABAQUS) modeling to monitor and interpret bottom-up reflective cracking. Rectangular and semi-cylindrical asphalt-overlaid PCC specimens were instrumented with surface-bonded distributed optical fibers in a serpentine layout with 20-mm spacing. Controlled bending tests reproduced bottom-up crack initiation and propagation, with cracks consistently originating at a predefined notch within the PCC layer and propagating toward the asphalt overlay. The OFDR-based DFOS system identified localized strain concentrations associated with crack development; and finite element simulations reproduced the observed crack initiation location, propagation path, stress redistribution, and global structural response. The close agreement among laboratory observations, distributed strain measurements, and numerical predictions validates the framework and demonstrates the potential of OFDR-based DFOS for structural health monitoring and condition assessment of rehabilitated concrete pavements.

17. Key Words	18. Distribution Statement
Distributed fiber optic sensing, Optical frequency domain reflectometry, Reflective cracking, PCC pavement, Asphalt overlay, Slab fracturing, Structural health monitoring, Finite element analysis	No restrictions. This document is available through the National Technical Information Service, Springfield, VA 22161.

19. Security Classif. (of this report)	20. Security Classif. (of this page)	21. No. of Pages	22. Price
Unclassified	Unclassified	51	n/a

Form DOT F 1700.7 (8-72) Reproduction of completed page authorized

CTIPS Center for Transformative Infrastructure Preservation and Sustainability

USDOT Region 8 University Transportation Center

Assessing Condition of Rehabilitated Concrete Pavement with Slab Fracturing and Asphalt Overlay Using Distributed Fiber Optic Sensors

Principal Investigator: Dr. Pan Lu
Upper Great Plains Transportation Institute
North Dakota State University

Authors

Dr. Pan Lu (PI)
Dr. Ying Huang (Co-PI)
Dr. Luyang Xu
Dr. Dawei Zhang
Yasir Mahmood

A report from

North Dakota State University
Upper Great Plains Transportation Institute
NDSU Dept 2880 • P.O. Box 6050
Fargo, ND 58108-6050
Phone: (701)231-7767
Website: https://www.ugpti.org/

August 2026

About the Center for Transformative Infrastructure Preservation and Sustainability

The Center for Transformative Infrastructure Preservation and Sustainability (CTIPS) is the U.S. DOT Region 8 University Transportation Center (UTC) located at North Dakota State University. CTIPS focuses on “preserving the existing transportation system,” along with consortia members Colorado State University, Fort Lewis College, South Dakota State University, United Tribes Technical College, University of Colorado Denver, University of Denver, University of North Dakota, University of Utah, University of Wyoming, and Utah State University.

Acknowledgements

This research was made possible by funding from the U.S. Department of Transportation through the Center for Transformative Infrastructure Preservation and Sustainability (CTIPS) and the Upper Great Plains Transportation Institute (UGPTI). The authors express their deep gratitude to U.S. DOT, CTIPS, and UGPTI.

U.S. Department of Transportation (US DOT) Disclaimer

The following publications resulted from the research conducted under this project, and acknowledgment was made to this project:

1. Mahmood Y, Xu L, Wang X, et al. “Embedded GFRP-packaged sensor system for real-time and high-precision vehicle load estimation in weigh-in-motion (WIM) applications[J].” *Measurement Science and Technology*, 2026, 37(9): 096004.

2. "A Hybrid Experimental–Numerical Framework for Monitoring Bottom-Up Reflective Cracking in Asphalt-Overlaid PCC Pavements Using OFDR-Based Distributed Fiber Optic Sensing" is under construction for a potential journal submission to *Applied Sciences, Special Issue: Advances in Intelligent Operation and Maintenance of Infrastructure*.

ABSTRACT

Reflective cracking is one of the primary causes of premature deterioration in asphalt-overlaid Portland cement concrete (PCC) pavements, reducing service life and increasing maintenance costs. Because crack initiation begins within the underlying PCC layer before becoming visible at the surface, conventional inspection methods have limited capability for early detection. This project developed and experimentally validated a hybrid experimental-numerical framework that integrates optical frequency domain reflectometry (OFDR)-based distributed fiber optic sensing (DFOS), laboratory-scale three-point bending tests, and finite element (ABAQUS) modeling to monitor and interpret bottom-up reflective cracking. Rectangular and semi-cylindrical asphalt-overlaid PCC specimens were instrumented with surface-bonded distributed optical fibers in a serpentine layout with 20-mm spacing. Controlled bending tests reproduced bottom-up crack initiation and propagation, with cracks consistently originating at a predefined notch within the PCC layer and propagating toward the asphalt overlay. The OFDR-based DFOS system identified localized strain concentrations associated with crack development; and finite element simulations reproduced the observed crack initiation location, propagation path, stress redistribution, and global structural response. The close agreement among laboratory observations, distributed strain measurements, and numerical predictions validates the framework and demonstrates the potential of OFDR-based DFOS for structural health monitoring and condition assessment of rehabilitated concrete pavements.

CONTENTS

1. INTRODUCTION AND BACKGROUND 1

2. LITERATURE REVIEW 4

2.1 Reflective Cracking in Asphalt-Overlaid PCC Pavements 4

2.2 Limitations of Surface-Based Pavement Monitoring 4

2.3 Embedded and Fiber Optic Sensing for Pavement Monitoring 5

2.4 Finite Element Modeling of Reflective Crack Propagation 5

2.5 Need for an Integrated Experimental–Numerical Monitoring Framework 6

2.6 Research Gaps 7

3. Methodology 8

3.1 Overview of the Proposed Framework 8

3.2 Laboratory Specimen Design 9

3.3 Distributed Fiber Optic Sensor Deployment and Crack Monitoring Layout 12

3.4 Experimental Procedure 15

3.5 Finite Element Modeling 16

3.6 Experimental–Numerical Validation Strategy 18

4. EXPERIMENTAL AND NUMERICAL ANALYSIS 20

4.1 Experimental Observation of Crack Initiation and Propagation 20

4.2 Distributed Strain Localization During Crack Propagation 21

4.3 Global Mechanical Response 23

4.4 DFOS Monitoring Results 25

4.5 Finite Element Analysis of Crack Initiation and Propagation 27

4.6 Experimental–Numerical Validation 29

5. SUMMARY 33

5.1 Major Contributions of this Study: 34

6. FUTURE RESEARCH 35

6.1 Cyclic and Fatigue Loading 35

6.2 Coupled Thermal and Environmental Effects 35

6.3 Interface Behavior and Slab-fracturing Treatments 35

6.4 Machine learning–assisted interpretation 35

7. REFERENCES 36

LIST OF FIGURES

Figure 1. Schematic illustration of the bottom-up reflective cracking mechanism in asphalt-overlaid Portland cement concrete (PCC) pavements. ... 3

Figure 2. Workflow of the proposed hybrid experimental–numerical framework ... 8

Figure 3. Geometry and dimensions of the laboratory-scale composite rectangular beam specimen ... 9

Figure 4. Geometry and dimensions of the laboratory-scale composite semi-cylindrical specimen ... 10

Figure 5. Artificial notch configurations used to promote bottom-up crack initiation in the (a) rectangular and (b) semi-cylindrical pavement specimens. The notch was introduced at the bottom center of the PCC layer to create a localized stress concentration and ensure consistent crack initiation during three-point bending... 11

Figure 6. Schematic illustration of the operating principle of OFDR-based distributed fiber optic sensing ... 13

Figure 7. Serpentine deployment layouts of the OFDR-based distributed fiber optic sensor for the (a) rectangular and (b) semi-cylindrical pavement specimens ... 14

Figure 8. Three-dimensional finite element models and loading configurations used for the numerical simulation of the (a) rectangular and (b) semi-cylindrical pavement specimens ... 17

Figure 9. Post-test fracture pattern of the rectangular asphalt-overlaid PCC specimen following three-point bending ... 20

Figure 10. Post-test fracture pattern of the semi-cylindrical asphalt-overlaid PCC specimen following three-point bending ... 21

Figure 11. Evolution of distributed strain along the sensing fiber in the rectangular specimen during three-point bending. Localized strain peaks correspond to sensing Lines 2–4 intersected by the propagating crack ... 22

Figure 12. Evolution of distributed strain along the sensing fiber in the semi-cylindrical specimen during three-point bending. Localized strain peaks indicate crack–fiber intersections along sensing Lines 2–4 ... 22

Figure 13. Experimental load–displacement responses of the rectangular and semi-cylindrical specimens subjected to three-point bending ... 24

Figure 14. Annotated post-test photograph of the rectangular asphalt-overlaid PCC specimen showing the surface-bonded DFOS sensing fibers, predefined notch, and bottom-up crack propagation path following three-point bending ... 25

Figure 15. Annotated post-test photograph of the semi-cylindrical asphalt-overlaid PCC specimen showing the DFOS sensing fiber layout and bottom-up crack propagation following three-point bending ... 26

Figure 16. Evolution of the tensile stress field predicted by the ABAQUS finite element model for the rectangular asphalt-overlaid PCC specimen during three-point bending. The three loading stages illustrate (a) elastic response, (b) crack initiation at the predefined notch, and (c) upward crack propagation accompanied by stress redistribution 27

Figure 17. Evolution of the tensile stress field predicted by the ABAQUS finite element model for the semi-cylindrical pavement specimen during three-point bending 28

Figure 18. Experimental–numerical validation of bottom-up reflective cracking in rectangular and semi-cylindrical pavement specimens. The figure compares (a) finite element tensile stress evolution, (b) experimentally observed crack propagation, and (c) global load–displacement responses obtained during three-point bending 30

LIST OF TABLES

Table 1. Geometric dimensions of the laboratory pavement specimens 10
Table 2. OFDR-based distributed fiber optic sensing configuration 14
Table 3. Experimental testing parameters... 16
Table 4. Material properties adopted in the finite element model 18
Table 5. Experimental–numerical validation criteria.. 19
Table 6. Summary of the experimental–numerical validation results 32

LIST OF KEY TERMS

ABAQUS – Commercial finite element analysis software used for numerical simulation.

Distributed fiber optic sensing (DFOS) – A sensing method in which the optical fiber acts as a continuous sensor along its length.

Finite element method (FEM) – A numerical method used to calculate stress, strain, deformation, and damage in structures.

Optical frequency domain reflectometry (OFDR) – A high-resolution optical interrogation method based on Rayleigh backscattering.

Portland cement concrete (PCC) – Hydraulic cement concrete commonly used in pavement construction.

Reflective cracking – Cracking that propagates from an underlying pavement discontinuity through an overlay.

Structural health monitoring (SHM) – Continuous or periodic monitoring used to assess structural condition and detect damage.

EXECUTIVE SUMMARY

This research addresses the need for early detection of reflective cracking in rehabilitated asphalt-overlaid concrete pavements, where bottom-up cracks initiate within the underlying concrete long before they become visible at the surface. The study develops and validates a hybrid experimental–numerical framework that integrates optical frequency domain reflectometry (OFDR)-based distributed fiber-optic sensing, laboratory three-point bending tests, and finite-element modeling to monitor crack initiation and propagation. Distributed sensors continuously captured localized strain evolution, while numerical simulations reproduced the observed fracture behavior and stress redistribution. By linking distributed strain measurements to experimentally validated finite element predictions, this research provides a reliable foundation for structural health monitoring and condition assessment of rehabilitated concrete pavements, supporting timelier, more cost-effective infrastructure preservation.

1. INTRODUCTION AND BACKGROUND

Portland cement concrete (PCC) pavements constitute a significant portion of highway transportation infrastructure due to their high structural capacity, long service life, and ability to withstand heavy traffic loads. As these pavements age, deterioration caused by repeated traffic loading, environmental effects, and material aging gradually reduces their structural performance [1, 2]. Rehabilitation is therefore an essential component of pavement management systems, allowing agencies to restore serviceability while minimizing construction costs and traffic disruption [3, 4]. Among available rehabilitation strategies, asphalt overlays remain among the most widely adopted solutions because they can be constructed rapidly, improve ride quality, and extend pavement service life without requiring complete pavement reconstruction [5, 6].

Despite these advantages, the long-term performance of asphalt-overlaid PCC pavements is frequently limited by reflective cracking [7]. Reflective cracks originate from existing joints, cracks, or other discontinuities in the underlying concrete pavement and progressively propagate through the asphalt overlay under repeated traffic loading and environmental actions [8, 9]. Once these cracks reach the pavement surface, they provide direct pathways for water infiltration, accelerate structural deterioration, and substantially increase maintenance requirements [10, 11]. Although numerous rehabilitation techniques, including slab fracturing, crack-and-seat, and rubblization, have been developed to reduce reflective cracking, complete elimination of this distress remains difficult because crack propagation is governed by complex interactions among pavement geometry, material properties, interface behavior, and cyclic loading [12, 13].

A fundamental challenge in mitigating reflective cracking is that damage initiates within the underlying pavement structure long before it becomes visible at the pavement surface [14, 15]. Consequently, the ability to identify bottom-up crack initiation at an early stage is critical for understanding pavement deterioration and developing effective maintenance strategies [16]. However, most pavement condition assessment techniques rely on surface observations and therefore provide limited information regarding the internal mechanical response responsible for crack development [2].

Conventional pavement inspection methods—including visual surveys, digital image processing, laser scanning, infrared thermography, ground-based imaging systems, and, more recently, AI-assisted crack detection—have significantly improved the efficiency and consistency of pavement condition assessment [16]. Nevertheless, these approaches primarily identify surface manifestations of distress after cracking has already developed. They cannot directly monitor the localized strain accumulation or internal fracture processes that precede visible damage. Embedded sensing technologies, such as electrical resistance strain gauges and fiber Bragg grating (FBG) sensors, provide direct measurements of structural response but remain limited to discrete sensing locations [17]. As a result, crack initiation may occur between adjacent sensors without being detected, making continuous monitoring of crack evolution challenging.

Distributed fiber optic sensing (DFOS) has emerged as a promising technology for structural health monitoring (SHM) because it enables continuous strain measurements along the entire length of an optical fiber with high spatial resolution [18]. Optical frequency domain reflectometry (OFDR)-based DFOS is particularly well suited for laboratory-scale structural investigations because it can accurately capture highly localized strain concentrations associated with crack initiation and propagation [19, 20]. Unlike conventional point sensors, distributed sensing does not require prior knowledge of the crack location, allowing the complete strain field to be monitored throughout the loading process [21]. Although recent studies have demonstrated the effectiveness of DFOS for monitoring concrete structures, composite materials, and transportation infrastructure, most investigations have focused primarily on sensing performance or strain measurement accuracy [22-24]. Comparatively fewer studies have integrated distributed strain measurements with physics-based numerical models capable of explaining the underlying fracture mechanisms responsible for crack development [12, 25-27].

Finite element modeling (FEM) provides a complementary tool for investigating internal stress redistribution, crack-tip behavior, and fracture evolution that cannot be directly measured during laboratory testing [28, 29]. When combined with experimental observations, numerical simulation provides a mechanistic interpretation of measured strain localization and enables direct investigation of the physical processes governing crack initiation and propagation [30, 31]. However, relatively few studies have established a comprehensive experimental–numerical framework that systematically integrates distributed fiber-optic measurements, laboratory observations, and finite-element predictions for rehabilitated asphalt-overlaid PCC pavements [32-34].

Based on the existing literature, four important knowledge gaps remain. First, current pavement monitoring techniques primarily identify damage after cracks become visible at the pavement surface rather than during the early stages of internal crack development. Second, conventional embedded sensors provide measurements only at discrete locations and therefore cannot continuously characterize strain evolution during crack propagation. Third, although OFDR-based DFOS offers continuous distributed strain measurements, its application to monitoring bottom-up reflective cracking in rehabilitated pavement systems remains limited. Finally, few studies have combined distributed fiber-optic sensing with experimentally validated finite-element modeling to establish a mechanistic understanding of reflective crack initiation and propagation.

To address these limitations, this study develops and experimentally validates a hybrid experimental–numerical framework for monitoring bottom-up reflective cracking in rehabilitated asphalt-overlaid PCC pavements. Laboratory-scale two-layer pavement specimens were instrumented with OFDR-based distributed fiber optic sensors and tested under three-point bending to monitor strain evolution during crack initiation and propagation. An experimentally validated FEM was developed to investigate the corresponding stress redistribution and fracture behavior. The central hypothesis of this study is that integrating DFOS with physics-based numerical modeling provides a reliable and mechanistically interpretable framework for detecting crack initiation, monitoring crack propagation, and elucidating the underlying fracture mechanisms before significant surface crack manifestation.

The primary contributions of this work are fourfold. First, a hybrid experimental–numerical framework integrating laboratory testing, OFDR-based DFOS, and FEM is developed to investigate bottom-up reflective cracking in rehabilitated pavement systems. Second, the study demonstrates the capability of DFOS to continuously monitor localized strain evolution associated with crack initiation and propagation. Third, experimentally validated finite element simulations are used to establish a direct relationship between measured strain localization and the internal stress redistribution governing fracture development. Finally, the proposed framework provides a scalable methodology for future field-scale SHM and condition assessment of rehabilitated pavement infrastructure. The physical mechanism governing bottom-up reflective cracking in rehabilitated pavement systems, from crack initiation at the existing PCC joint to crack propagation through the asphalt overlay under traffic loading, is illustrated in Figure 1.

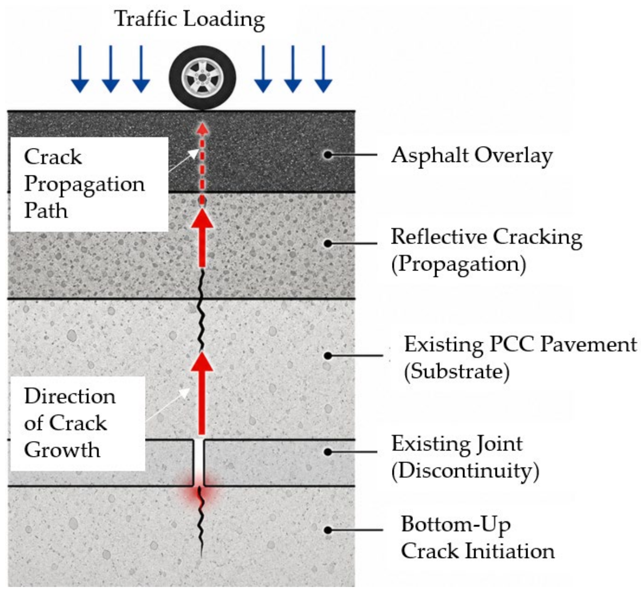

Figure 1. Schematic illustration of the bottom-up reflective cracking mechanism in asphalt-overlaid Portland cement concrete (PCC) pavements

2. LITERATURE REVIEW

2.1 Reflective Cracking in Asphalt-Overlaid PCC Pavements

Asphalt overlays are widely used to rehabilitate deteriorated PCC pavements because they improve ride quality, restore surface condition, and extend pavement service life without requiring full reconstruction [35]. However, the long-term performance of asphalt-overlaid PCC pavements is frequently limited by reflective cracking. Reflective cracking occurs when joints, cracks, or discontinuities in the existing PCC layer generate stress concentrations that propagate upward through the asphalt overlay under traffic loading and environmental effects [15].

The reflective cracking mechanism is governed by the interaction among the existing concrete slab, the asphalt overlay, and their interface. Under repeated wheel loading, vertical deflection and horizontal movement at existing PCC joints produce tensile and shear stresses near the bottom of the overlay and at the asphalt–PCC interface [9]. Over time, these stresses initiate cracks that grow upward toward the surface. Once the crack reaches the surface, water infiltration, oxidation, freeze–thaw damage, and traffic-induced deterioration accelerate the loss of structural capacity [36, 37].

Slab-fracturing techniques, including crack-and-seat, break-and-seat, and rubblization, are commonly applied before asphalt overlay placement to reduce slab length, minimize joint movement, and decrease stress concentration at existing discontinuities [35, 38, 39]. Although these methods can delay reflective cracking, they do not eliminate the need to monitor crack initiation and propagation within the pavement structure. The effectiveness of slab-fracturing treatments depends on material properties, fracture pattern, overlay thickness, bonding condition, traffic loading, and environmental exposure [40]. Therefore, reliable monitoring of internal crack development is essential for evaluating the long-term performance of rehabilitated pavement systems.

2.2 Limitations of Surface-Based Pavement Monitoring

Conventional pavement condition assessment relies primarily on surface-based inspection methods, including visual surveys, digital imaging, laser crack measurement systems, three-dimensional laser scanning, infrared thermography, and unmanned aerial vehicle-based imaging [41-43]. Recent advances in AI and computer vision have improved the automated detection and classification of visible pavement distress such as cracking, rutting, potholes, and surface defects [44, 45]. These methods are valuable for network-level condition assessment because they provide rapid, repeatable, and large-scale pavement inspection.

Despite these advantages, surface-based monitoring methods are inherently limited in their ability to detect early-stage reflective cracking. Bottom-up reflective cracking initiates within the underlying PCC layer or near the asphalt–PCC interface before reaching the pavement surface [36, 44]. As a result, surface inspection methods can only identify the distress after the internal crack has already propagated through a significant portion of the pavement structure [15, 46]. This delay limits transportation agencies' ability to implement preventive maintenance before damage becomes severe.

Surface-based approaches also provide limited information about the mechanical processes responsible for crack growth [47]. Image-based and laser-based methods can quantify surface crack length, width, and pattern, but they do not directly measure internal strain accumulation, stress redistribution, or crack-tip behavior [48, 49]. Therefore, while surface monitoring technologies are effective for supporting visible distress, they are insufficient for understanding the initiation and early propagation of bottom-up cracking in rehabilitated asphalt-overlaid PCC pavements.

2.3 Embedded and Fiber Optic Sensing for Pavement Monitoring

To overcome the limitations of surface inspection, embedded sensing technologies have been investigated for pavement structural health monitoring. Conventional strain gauges, piezoelectric sensors, accelerometers, and acoustic emission sensors can provide direct measurements of structural response under loading [50-52]. However, these sensors are generally limited to discrete measurement locations. Their performance depends strongly on sensor placement, and they may fail to detect damage if cracking occurs away from the instrumented location [53].

Fiber optic sensors offer several advantages for pavement monitoring, including high sensitivity, corrosion resistance, immunity to electromagnetic interference, small size, and compatibility with long-term monitoring applications [2, 54]. FBG sensors have been used to measure internal strain and detect crack development in pavement and concrete specimens [55]. However, FBG sensors remain point-based or quasi-distributed systems because measurements are obtained only at grating locations. To capture distributed crack development, dense sensor arrays are required, which increase costs, installation complexity, and data management requirements.

DFOS addresses this limitation by converting the optical fiber itself into a continuous sensing element. Depending on the interrogation method, DFOS can measure strain or temperature along the entire fiber length, allowing spatially continuous monitoring of structural response [56]. Among DFOS techniques, OFDR based on Rayleigh backscattering is particularly suitable for laboratory-scale crack monitoring because it provides high spatial resolution and can identify localized strain concentrations associated with crack initiation and propagation [19, 57].

DFOS's ability to measure continuous strain fields makes it highly relevant for reflective cracking applications. Because the exact location of crack initiation is generally unknown, a distributed sensing path provides greater reliability in damage detection than isolated point sensors. Localized strain peaks measured by DFOS can indicate crack initiation, crack opening, and stress redistribution around the crack path [58]. However, interpreting DFOS measurements in layered asphalt–PCC systems remains technically challenging. Measured strain fields may be influenced by bonding quality, fiber layout, material heterogeneity, interface behavior, crack opening displacement, and flexural deformation. Therefore, DFOS data must be interpreted within a mechanics-based framework rather than treated only as sensing output.

2.4 Finite Element Modeling of Reflective Crack Propagation

FEM has been widely used to investigate reflective cracking and fracture behavior in pavement systems [59]. Numerical models enable researchers to evaluate stress distributions, strain concentrations, interface behavior, crack-tip responses, and crack propagation under controlled loading and material conditions. For asphalt-overlaid PCC pavements, finite element studies have shown that reflective cracking is strongly affected by overlay thickness, PCC joint movement, interface bonding, temperature, material stiffness, and loading position [60].

Fracture mechanics-based numerical approaches, including cohesive zone modeling, extended finite element methods, damage mechanics, and concrete damaged plasticity, have been applied to simulate crack initiation and propagation in pavement materials [61]. These models can provide insight into internal mechanisms that are difficult or impossible to measure experimentally, such as tensile stress concentration near the notch, stress redistribution around an advancing crack tip, and damage evolution near the asphalt–PCC interface [62].

However, numerical models require experimental validation because their predictions depend on assumptions regarding material behavior, boundary conditions, interface properties, crack geometry, and damage criteria. Many pavement fracture studies validate FEMs using global responses such as load–displacement curves, surface crack patterns, or limited strain measurements [4]. While useful, these validation methods provide incomplete information about the spatial distribution of internal strain and damage. A model may reproduce the global load–displacement response while still misrepresenting the local strain field around the crack tip [63].

This limitation is especially important for reflective cracking, where localized strain concentration and crack-tip behavior govern damage initiation. Distributed strain measurements from DFOS provide a unique opportunity to validate finite element predictions at a much higher spatial resolution than conventional point sensors. By comparing measured strain localization with numerically predicted stress concentrations and crack-propagation patterns, the numerical model can be evaluated not only at the structural response level but also at the local fracture-mechanics level.

2.5 Need for an Integrated Experimental–Numerical Monitoring Framework

The reviewed literature highlights that surface inspection, embedded sensing, distributed sensing, and FEM each provide useful but incomplete information for evaluating reflective cracking. Surface inspection can document visible distress but cannot detect internal crack initiation. Point sensors can measure local structural response but may miss cracks between sensor locations. DFOS can capture continuous strain fields but requires mechanics-based interpretation to relate strain localization to crack growth. FEM can explain stress redistribution and fracture behavior but requires spatially detailed experimental validation.

These limitations suggest the need for an integrated framework that combines the strengths of experimental monitoring and numerical simulation. In such a framework, laboratory testing provides controlled crack initiation and observable fracture behavior; DFOS provides continuous distributed strain measurements during crack evolution; and finite element modeling provides a mechanical interpretation of the measured strain field. Comparing experimental crack observations, DFOS strain localization, and finite-element stress predictions can establish a direct relationship between sensing responses and fracture mechanisms.

For rehabilitated asphalt-overlaid PCC pavements, this integration is particularly important because bottom-up cracking develops internally before it manifests at the surface. A hybrid experimental–numerical framework can therefore support both early crack detection and mechanistic interpretation of damage progression. Such an approach is necessary for moving beyond simple crack observation toward structural health monitoring methods that can identify damage initiation and track propagation and explain the physical processes governing reflective cracking.

2.6 Research Gaps

Based on the reviewed literature, four specific research gaps motivate the present study.

- Most pavement monitoring methods detect reflective cracking only after the distress becomes visible at the pavement surface. These methods provide limited ability to identify the early internal damage stage, where preventive maintenance would be most effective.
- Conventional embedded sensors, including strain gauges and FBG sensors, provide measurements only at discrete locations. This limits their ability to continuously monitor spatially distributed crack initiation and propagation in rehabilitated pavement systems.
- Although OFDR-based DFOS provides continuous high-resolution strain measurements, its application to bottom-up reflective cracking in asphalt-overlaid slab-fractured PCC pavements remain limited. In particular, the relationship between DFOS strain localization and actual crack propagation behavior has not been sufficiently established for layered pavement specimens.
- Finite element models of reflective cracking often lack validation using spatially continuous strain measurements. As a result, the connection between numerical stress predictions, measured distributed strain fields, and experimentally observed crack evolution remains underdeveloped.

To address these gaps, this study develops a hybrid experimental–numerical framework that integrates laboratory testing, OFDR-based DFOS monitoring, and FEM to investigate bottom-up crack initiation and propagation in two-layer asphalt–PCC specimens representative of rehabilitated slab-fractured pavement systems. The proposed framework is designed to detect localized strain evolution during crack development and to interpret the measured response through experimentally validated numerical simulation.

3. METHODOLOGY

3.1 Overview of the Proposed Framework

This study employs a hybrid experimental numerical framework to investigate the initiation and propagation of bottom-up reflective cracking in rehabilitated asphalt-overlaid PCC pavements. The framework integrates controlled laboratory experiments, OFDR-based DFOS, and FEM to establish a direct relationship between experimentally observed crack development, distributed strain localization, and the underlying stress redistribution governing fracture propagation. By combining continuous strain measurements with physics-based numerical analysis, the proposed methodology offers both early crack detection and a mechanistic interpretation of reflective cracking. The overall research workflow is illustrated in Figure 2.

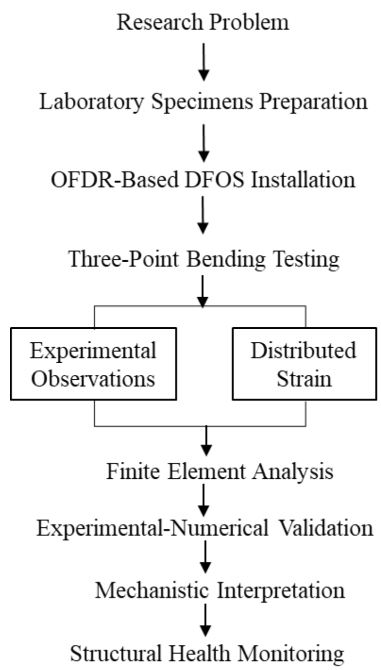

Figure 2. Workflow of the proposed hybrid experimental–numerical framework

The investigation began with the engineering problem of reflective cracking in rehabilitated pavement systems. Laboratory-scale two-layer asphalt–PCC specimens were then fabricated to reproduce the structural characteristics of rehabilitated pavements and instrumented with OFDR-based DFOS using a serpentine deployment configuration. Controlled three-point bending tests were subsequently conducted while continuously recording load, displacement, distributed strain, and crack development. The experimentally measured responses were used to develop and validate an FEM capable of simulating the corresponding stress distribution and fracture behavior. Finally, the experimental observations and numerical predictions were integrated to establish a mechanistic understanding of bottom-up crack propagation and to demonstrate the applicability of the proposed framework for future structural health monitoring of rehabilitated pavement infrastructure.

Unlike conventional experimental studies, in which sensing and numerical analysis are performed independently, the present framework integrates laboratory observations, distributed strain measurements, and finite element simulations into a unified validation process. This integration enabled experimentally measured strain localization to be directly related to internal stress redistribution and crack evolution, thereby providing a more comprehensive understanding of reflective cracking mechanisms.

The distinguishing feature of the proposed framework is the direct integration of distributed strain measurements with finite element predictions. Rather than treating experimental sensing and numerical simulation as independent analyses, the framework established a closed-loop validation process in which experimentally observed crack development, measured strain localization, and simulated stress fields are evaluated simultaneously.

3.2 Laboratory Specimen Design

Representative laboratory specimens are essential for investigating the mechanisms governing bottom-up reflective cracking under controlled and repeatable conditions. Although full-scale pavement testing provides the most realistic representation of in-service pavement behavior, laboratory-scale specimens offer a practical, highly repeatable platform for isolating the factors influencing crack initiation and propagation. Accordingly, two-layer composite pavement specimens were designed to reproduce the structural characteristics of rehabilitated asphalt-overlaid PCC pavements while remaining compatible with OFDR-based DFOS and laboratory-scale mechanical testing.

Each specimen consisted of an asphalt overlay bonded to an underlying PCC layer, representing the rehabilitation overlay and the existing concrete pavement, respectively. This two-layer configuration preserves the fundamental structural interaction between the asphalt overlay and the PCC substrate, enabling the fracture mechanisms associated with bottom-up reflective cracking to be investigated under controlled flexural loading conditions. Two specimen geometries were adopted in this study: a rectangular beam specimen and a semi-cylindrical specimen, as shown in Figures 3 and 4.

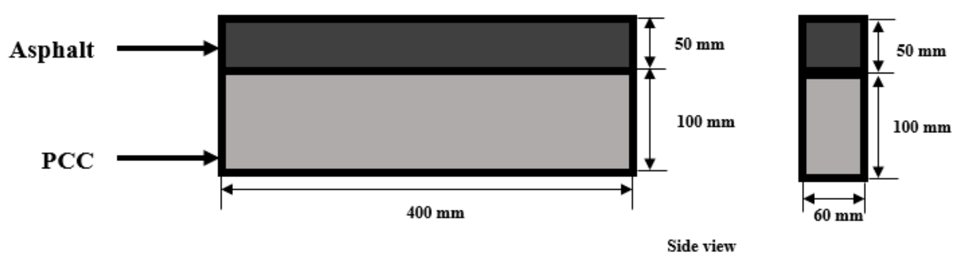

Figure 3. Geometry and dimensions of the laboratory-scale composite rectangular beam specimen

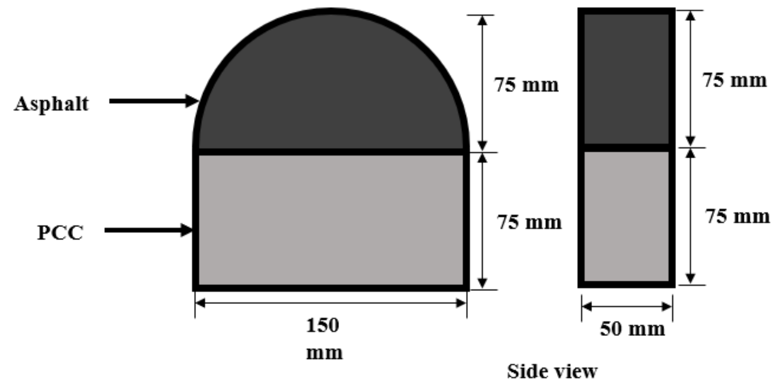

Figure 4. Geometry and dimensions of the laboratory-scale composite semi-cylindrical specimen

The rectangular specimen provides a conventional geometry for three-point bending tests and serves as a reference configuration for evaluating crack initiation and propagation. The semi-cylindrical specimen was introduced to examine the applicability of the proposed monitoring framework under a different structural geometry with a modified stress distribution. Maintaining identical material composition and layer thicknesses in both configurations allows the influence of specimen geometry on strain localization and fracture behavior to be evaluated independently of material properties.

The rectangular specimen consisted of a 50-mm asphalt overlay bonded to a 100-mm PCC layer, yielding an overall size of 400 mm × 60 mm × 150 mm. The semi-cylindrical specimen comprised a 75-mm asphalt overlay bonded to a 75-mm PCC layer, resulting in an overall specimen diameter of 150 mm, a total height of 150 mm, and a specimen thickness of 50 mm. These dimensions were selected to satisfy three engineering objectives: (i) to reproduce the structural interaction between the asphalt overlay and the PCC substrate at the laboratory scale; (ii) to ensure compatibility with the loading capacity and span limitations of the three-point bending apparatus; and (iii) to provide sufficient surface area for installing the serpentine distributed fiber optic sensing layout while maintaining adequate spatial resolution for distributed strain monitoring. The dimensions of both specimen configurations are summarized in Table 1.

Table 1. Geometric dimensions of the laboratory pavement specimens

Specimen	Geometry	Asphalt Thickness (mm)	PCC Thickness (mm)	Overall Dimensions
Rectangular	Beam	50	100	400 × 60 × 150 mm
Semi-cylindrical	Semi-cylinder	75	75	Diameter = 150 mm; Height = 150 mm; Thickness = 50 mm

For a simply supported beam subjected to three-point bending, the maximum bending moment is given by [64, 65].

$$M_{max} = PL/4 \quad (1)$$

where (P) is the applied load and (L) is the support span. The corresponding flexural stress distribution across the specimen depth is expressed as [66, 67].

$$\sigma = My/I \tag{2}$$

Where σ is the bending stress, (M) is the bending moment, (y) is the distance from the neutral axis, and (I) is the second moment of area. Equation (2) indicates that the maximum principal tensile stress develops at the bottom of the specimen, making this location the most susceptible to crack initiation during flexural loading. This mechanical behavior provides the basis for introducing a predefined notch at the bottom of the PCC layer.

These equations indicate that the maximum principal tensile stress occurs at the bottom surface of the specimen, which justifies placing the artificial notch to promote controlled bottom-up crack initiation.

To promote consistent crack initiation, artificial notches were machined at the bottom center of each specimen, as illustrated in Figure 5. For the rectangular specimens, a 25-mm-deep rectangular notch, corresponding to approximately one-quarter of the PCC layer thickness, was introduced. For the semi-cylindrical specimens, a 56-mm-deep notch, equivalent to approximately three-quarters of the 75-mm PCC layer thickness, was used. In both geometries, the notch served as a predefined crack initiation site by increasing the local tensile stress concentration at the bottom of the concrete layer during flexural loading.

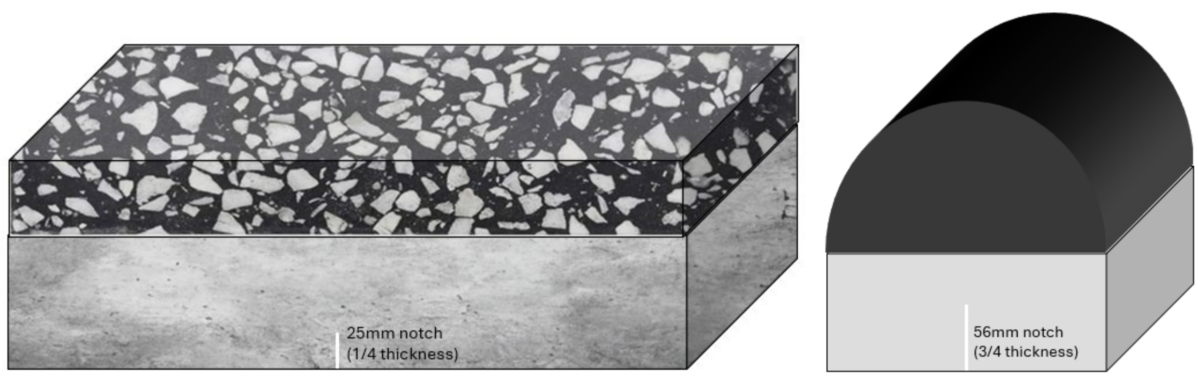

Figure 5. Artificial notch configurations used to promote bottom-up crack initiation in the (a) rectangular and (b) semi-cylindrical pavement specimens. The notch was introduced at the bottom center of the PCC layer to create a localized stress concentration and ensure consistent crack initiation during three-point bending.

Introducing the notch at a known location reduced variability in crack initiation across repeated tests and ensured that fractures consistently initiated at the bottom of the PCC layer. This allowed a direct comparison of visual crack observations, distributed strain measurements from the OFDR-based DFOS system, and finite element predictions. The notch geometry was selected to generate sufficient stress concentration without causing premature failure prior to the onset of controlled flexural loading.

The specimen geometries and notch configurations adopted in this study provide a reliable experimental platform for investigating bottom-up reflective cracking under laboratory conditions. By maintaining consistent crack initiation while accommodating distributed strain measurements and numerical simulations, the specimens enable systematic evaluation of crack development and facilitate direct correlation between experimental observations and finite-element analysis.

3.3 Distributed Fiber Optic Sensor Deployment and Crack Monitoring Layout

Continuous monitoring of strain evolution during crack initiation and propagation was achieved using OFDR-based DFOS. Unlike conventional electrical resistance strain gauges, which provide measurements only at discrete locations, DFOS utilizes the entire optical fiber as a continuous sensing element, enabling strain to be measured at thousands of closely spaced points along a single fiber. This distributed sensing capability provides high spatial resolution and allows localized deformation associated with crack initiation and propagation to be detected without prior knowledge of the crack location. Consequently, OFDR-based DFOS is particularly well suited for monitoring bottom-up reflective cracking in layered pavement systems, where the precise location of crack initiation cannot be predetermined.

The operating principle of OFDR is based on Rayleigh backscattering within the optical fiber. A swept-frequency laser generated by the OFDR interrogator is transmitted through the sensing fiber, producing a unique Rayleigh backscattering signature along its entire length. When the fiber undergoes mechanical deformation or temperature variation, localized changes in the optical path length result in measurable shifts in the backscattered spectrum. By comparing the measured spectrum with the reference spectrum obtained before loading, the distributed strain along the sensing fiber can be determined.

The relationship between the normalized wavelength shift and the corresponding strain and temperature variations is expressed as [11, 20]

$$\Delta\lambda/\lambda = KT\Delta T + K_{\varepsilon}\varepsilon \tag{3}$$

Where $\Delta\lambda$ is the measured wavelength shift, λ is the reference wavelength, KT and $K\varepsilon$ are the temperature and strain calibration coefficients, ΔT is the temperature variation, and ε is the mechanical strain.

Because all experiments were conducted under controlled laboratory conditions with negligible temperature fluctuations, the temperature-induced wavelength shift was assumed to be insignificant. Consequently, Equation (3) reduces to

$$\Delta\lambda/\lambda = K_{\varepsilon}\varepsilon \tag{4}$$

indicating that the measured wavelength shifts are directly proportional to the mechanically induced strain within the pavement specimen. Figure 6 illustrates the operating principle of the OFDR-based distributed sensing system. The swept laser generates a reference Rayleigh backscattering signature along the sensing fiber.

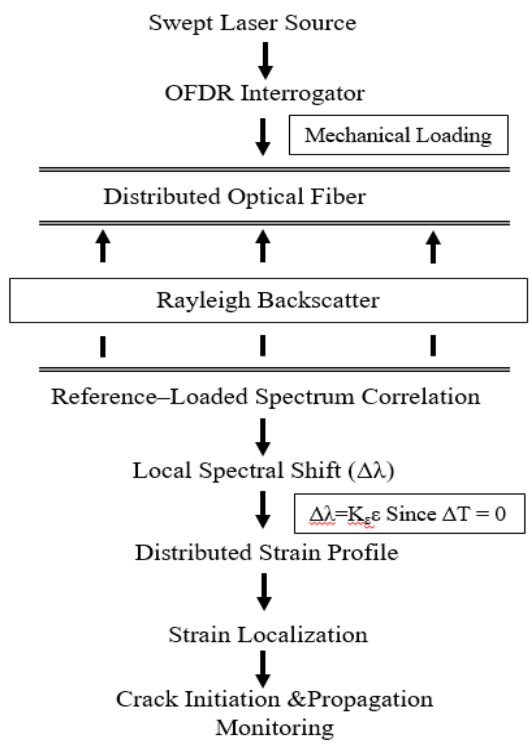

Figure 6. Schematic illustration of the operating principle of OFDR-based distributed fiber optic sensing

During mechanical loading, localized wavelength shifts induced by deformation are continuously converted into distributed strain measurements, enabling real-time monitoring of crack initiation and propagation.

To maximize sensing coverage within the anticipated crack propagation region, the optical fiber was surface bonded to each pavement specimen using a serpentine deployment configuration, as illustrated in Figure 7. Compared with a conventional straight fiber layout, the serpentine arrangement substantially increases the monitored area while maintaining a single continuous sensing path. This configuration increases the probability of capturing localized strain concentrations, regardless of the exact crack initiation location, and provides continuous strain information throughout the fracture process.

Different sensing layouts were designed for the two specimen geometries while maintaining comparable monitoring coverage. For the rectangular specimens, the sensing fiber was arranged in parallel horizontal paths with an approximately 20-mm spacing between adjacent sensing lines, covering the region expected to experience the highest tensile stresses during three-point bending. For the semi-cylindrical specimens, the fiber followed the specimen curvature using an equivalent serpentine arrangement with the same nominal spacing. In both configurations, the sensing paths were concentrated within the lower portion of the specimen where crack initiation was expected according to flexural beam theory.

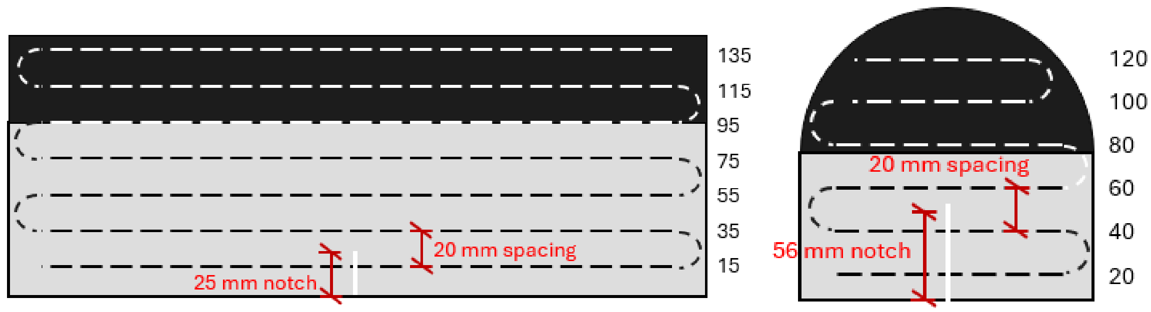

Figure 7. Serpentine deployment layouts of the OFDR-based distributed fiber optic sensor for the (a) rectangular and (b) semi-cylindrical pavement specimens

Prior to testing, the sensing fiber was bonded to the specimen surface using a high-strength adhesive to ensure efficient strain transfer between the pavement material and the optical fiber. After installation, an initial reference scan was acquired under unloaded conditions to establish the baseline Rayleigh backscattering signature. During the three-point bending tests, the OFDR interrogator continuously recorded distributed strain along the sensing fiber while the applied load and actuator displacement were simultaneously acquired by the material testing system (MTS). The synchronized acquisition of mechanical and optical measurements enabled direct correlation between structural response, strain localization, and crack development throughout the loading process. A summary of the distributed sensing configuration adopted in this study is provided in Table 2.

Table 2. OFDR-Based Distributed Fiber Optic Sensing Configuration

Parameter	Specification
Sensing technology	Optical frequency domain reflectometry (OFDR)
Sensor type	Distributed optical fiber
Measurement quantity	Distributed strain
Fiber installation	Surface bonded
Deployment pattern	Serpentine
Spacing between sensing paths	Approximately 20 mm
Reference measurement	Unloaded condition
Data acquisition	Continuous during loading
Temperature compensation	Neglected under laboratory-controlled conditions
Monitoring objective	Bottom-up crack initiation and propagation

The sensing configuration summarized in Table 2 was selected to provide a balance between monitoring coverage, measurement resolution, and practical installation requirements. The approximately 20-mm spacing between adjacent sensing paths was sufficient to capture localized strain gradients associated with crack initiation while avoiding unnecessary sensor redundancy. The distributed strain measurements obtained from the OFDR system constitute the primary experimental dataset used throughout this study to characterize crack initiation, strain localization, and fracture propagation. These measurements are subsequently compared with finite element predictions to establish a mechanistic interpretation of the observed fracture behavior and to validate the proposed hybrid experimental–numerical framework.

3.4 Experimental Procedure

Three-point bending tests were conducted to investigate the initiation and propagation of bottom-up reflective cracking under controlled laboratory conditions. The experimental program was designed to reproduce the flexural stress state responsible for crack development in rehabilitated asphalt-overlaid PCC pavements while simultaneously monitoring the structural response and distributed strain evolution. By combining mechanical loading with OFDR-based DFOS, the experimental procedure enabled continuous monitoring of localized strain development throughout the fracture process.

The system consisted of a servo-controlled MTS for applying the mechanical load, an OFDR interrogator connected to the distributed optical fiber, and a digital imaging system for documenting crack development. The specimens were tested under a simply supported three-point bending configuration, producing maximum principal tensile stresses at the bottom of the PCC layer where the predefined notch was introduced. This loading arrangement promotes controlled bottom-up crack initiation while providing a repeatable loading condition for comparing different specimen geometries.

Prior to testing, the distributed optical fiber was bonded to the specimen surface using the serpentine sensing layout described in Section 3.3. Each specimen was then positioned on the loading frame with simply supported boundary conditions and carefully aligned to ensure symmetric load application. Before mechanical loading commenced, an initial OFDR reference scan was acquired under unloaded conditions to establish the baseline Rayleigh backscattering signature for subsequent distributed strain measurements.

Mechanical loading was applied under displacement-controlled conditions using the servo-controlled MTS. Throughout the test, the applied load and actuator displacement were continuously recorded by the MTS data acquisition system, while the OFDR interrogator simultaneously measured the distributed strain along the entire sensing fiber. The synchronized acquisition of mechanical and optical data enabled localized strain evolution to be monitored continuously from the onset of loading until specimen failure. The principal experimental parameters adopted in this study are summarized in Table 3.

Table 3. Experimental testing parameters

Parameter	Value
Interrogator	Luna ODiSI-B
Sensing technology	OFDR
Fiber type	SMF-28
Gauge pitch	0.65 mm
Spatial resolution	0.65 mm
Installation	Surface bonded
Layout	Serpentine
Fiber spacing	20 mm
Temperature compensation	Neglected
Data acquisition	Continuous

Crack initiation and propagation were independently documented using high-resolution digital imaging throughout the loading process. Images were captured at selected loading intervals to record crack initiation, crack trajectory, crack opening, and penetration through the asphalt–PCC interface. Following completion of each test, crack widths were measured at multiple locations along the crack path to quantify the variation in crack opening through the specimen depth. These image-based measurements provided an independent dataset for comparison with the distributed strain measurements obtained from the OFDR system.

The experimental program generated three complementary datasets describing the fracture behavior of the layered pavement specimens. The MTS provided the global load–displacement response, the OFDR system supplied continuous distributed strain measurements, and the digital images documented the physical evolution of crack initiation and propagation. Together, these datasets form the experimental basis for evaluating bottom-up reflective cracking and for validating the finite element model presented in the following section.

3.5 Finite Element Modeling

To complement the laboratory investigation and provide a mechanistic interpretation of bottom-up reflective cracking, a three-dimensional FEM was developed in ABAQUS. The numerical model was designed to reproduce the laboratory three-point bending tests by replicating the specimen geometry, material configuration, notch geometry, loading arrangement, and boundary conditions. While the experimental program provides direct observations of crack initiation and distributed strain evolution, the FEM enables evaluation of the internal stress redistribution and strain fields that cannot be directly measured during testing. Together, the experimental and numerical approaches form the proposed hybrid experimental–numerical framework.

Separate FEMs were developed for the rectangular and semi-cylindrical pavement specimens described in Section 3.2. Each model reproduces the specimen geometry, asphalt overlay, PCC layer, predefined notch, loading nose, and support rollers used during the laboratory three-point bending tests. This ensures direct correspondence between the numerical simulations and the experimental configuration. Figure 8 illustrates the three-dimensional finite element models developed in ABAQUS for the two specimen geometries.

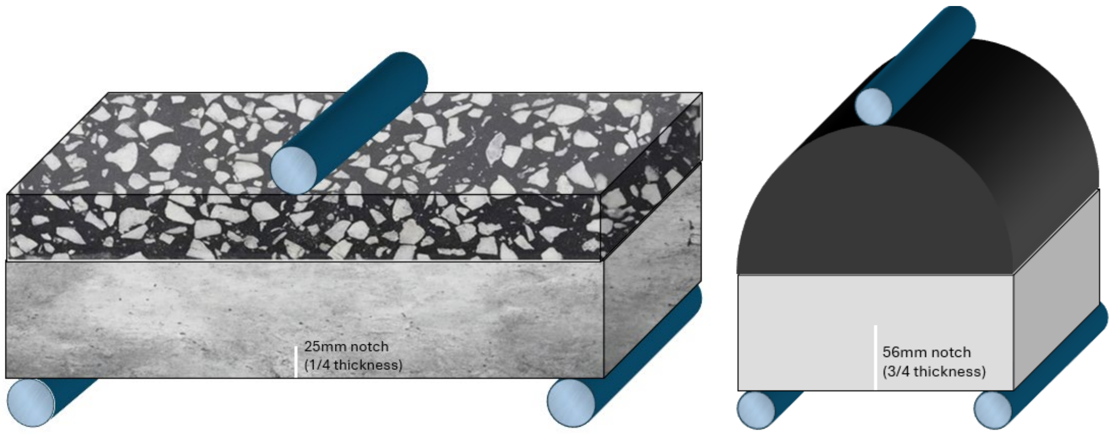

Figure 8. Three-dimensional finite element models and loading configurations used for the numerical simulation of the (a) rectangular and (b) semi-cylindrical pavement specimens.

The loading nose and support rollers were modeled as rigid cylindrical bodies, while displacement-controlled loading was applied at the specimen mid-span to reproduce the laboratory testing conditions. Both specimen ends were supported using simply supported boundary conditions, thereby generating tensile stresses within the lower portion of the PCC layer where crack initiation was experimentally observed.

The numerical simulations were performed under quasi-static loading conditions. The equilibrium of the solid domain is governed by

$$\nabla \cdot \sigma + b = 0 \quad (5)$$

Where: σ is the Cauchy stress tensor, and b is the body force vector per unit volume.

The strain–displacement relationship is given by

$$\varepsilon = 1/2(\nabla u + (\nabla u)T) \quad (6)$$

Where: ε is the strain tensor, and u is the displacement vector.

For the elastic portion of the material response, the stress–strain relationship can be written as

$$\Sigma = (1 - d)\, D_0 \varepsilon \quad (7)$$

where d is the scalar damage variable, D_0 is the undamaged elastic stiffness matrix, and ε is the strain tensor. These governing equations form the mechanical basis for evaluating stress redistribution, strain localization, and fracture evolution within the layered pavement system.

The asphalt overlay and PCC layer were assigned independent material properties to represent their distinct mechanical characteristics. Both asphalt and PCC were modeled as isotropic homogeneous elastic materials for the purpose of evaluating stress redistribution during laboratory-scale loading. Material parameters were obtained from laboratory characterization and published literature representative of asphalt mixtures and PCC used in pavement rehabilitation. The material properties adopted in the numerical simulations are summarized in Table 4.

Table 4. Material properties adopted in the finite element model

Property	Asphalt Overlay	PCC Layer
Young's modulus, E (GPa)	5.515	32.1
Poisson's ratio	0.35	0.2
Density (kg/m³)	2,300	2,200
Compressive strength (MPa)	1.4	35.8
Tensile strength (MPa)	0.9	3

A perfect bond was assumed between the asphalt overlay and the PCC layer using a tie constraint, ensuring full displacement compatibility across the interface throughout the analysis. This assumption is consistent with the laboratory specimens, where no visible interfacial debonding was observed during testing. Consequently, the numerical analysis focused exclusively on the initiation and propagation of bottom-up cracking within the layered pavement system.

The three-point bending tests were reproduced numerically by applying a displacement-controlled load at the specimen mid-span while constraining the support rollers using simply supported boundary conditions. The displacement-controlled loading procedure is consistent with the experimental methodology and enables stable simulation of progressive stiffness degradation during crack initiation and propagation. The primary model outputs included reaction force, displacement, maximum principal stress, tensile strain, and damage evolution.

A structured mesh refinement strategy was adopted in the vicinity of the predefined notch to accurately capture the high stress gradients associated with crack initiation. A comparatively coarser mesh was employed in regions remote from the notch to reduce computational cost while maintaining solution accuracy. A mesh sensitivity study was performed to verify that further refinement produced negligible changes in the predicted load–displacement response and crack initiation location.

The FEM provides the numerical component of the proposed hybrid framework by quantifying the internal stress and strain fields that govern bottom-up reflective cracking. The numerical predictions are subsequently compared with the experimental observations and distributed strain measurements to evaluate the capability of the proposed monitoring approach, as described in Section 3.6.

3.6 Experimental–Numerical Validation Strategy

The proposed hybrid experimental–numerical framework was validated by comparing independent datasets obtained from laboratory testing, OFDR-based DFOS, and finite element analysis. The objective of this validation strategy is to assess the capability of the numerical model to reproduce the experimentally observed structural response and fracture behavior while verifying that the distributed strain measurements accurately represent the evolution of bottom-up reflective cracking.

Model validation was performed using four complementary criteria that evaluate both the global mechanical response and the localized fracture characteristics of the pavement specimens.

The first validation criterion compares the load–displacement response obtained from the MTS with the corresponding finite element predictions. This comparison evaluates the ability of the numerical model to reproduce the overall stiffness, peak load, and structural response of the layered pavement specimens under three-point bending.

The second criterion examines crack initiation and propagation. The experimentally observed crack initiation location, propagation path, and penetration through the asphalt–PCC system are compared with the crack evolution predicted by the finite element model. This comparison assesses whether the numerical model accurately represents the fracture mechanisms governing bottom-up reflective cracking.

The third validation criterion focuses on distributed strain measurements obtained from the OFDR-based DFOS system. Localized strain concentrations measured during laboratory testing are compared with the tensile stress and strain distributions predicted by the finite element analysis. Particular emphasis is placed on the spatial correspondence between experimentally measured strain localization and the predicted stress concentration surrounding the crack tip.

The fourth criterion evaluates the crack-width distribution measured after testing. Crack widths recorded at different locations along the crack path are compared with the numerical damage distribution to assess the progression of fracture through the specimen thickness and to verify the consistency of the predicted crack development. The four validation criteria adopted in this study are summarized in Table 5.

Table 5. Experimental–numerical validation criteria

Validation criterion	Experimental measurement	Numerical prediction
Global response	Load–displacement curve	Load–displacement curve
Crack initiation	Crack initiation location	Predicted crack initiation
Crack propagation	Crack trajectory	Predicted crack path
Distributed strain	OFDR strain localization	Stress/strain concentration
Crack width	Measured crack-width distribution	Damage distribution

The combined use of these complementary validation criteria provides a comprehensive assessment of the proposed hybrid framework by integrating global structural response, distributed strain measurements, crack development, and numerical predictions. The application of this validation strategy and the corresponding results are presented in Section 4.

4. EXPERIMENTAL AND NUMERICAL ANALYSIS

4.1 Experimental Observation of Crack Initiation and Propagation

The three-point bending experiments successfully reproduced the bottom-up reflective cracking mechanism commonly observed in rehabilitated PCC pavements with asphalt overlays. In all tested specimens, crack initiation consistently occurred at the predefined notch located at the bottom of the PCC layer, confirming that the specimen geometry and loading configuration generated the intended tensile stress concentration. Following crack initiation, the fracture propagated upward through the PCC layer toward the asphalt overlay, reproducing the characteristic bottom-up crack development observed in field pavements.

The post-test fracture pattern of the rectangular specimen is shown in Figure 9. Crack initiation occurred directly above the predefined notch, after which the fracture propagated almost vertically along the specimen centerline. The nearly straight crack trajectory indicates that fracture propagation was dominated by tensile opening (Mode-I fracture) under the symmetric three-point bending configuration. No significant lateral deviation or branching was observed, demonstrating that the loading arrangement produced a stable and repeatable fracture path.

Figure 9. Post-test fracture pattern of the rectangular asphalt-overlaid PCC specimen following three-point bending

The corresponding fracture pattern for the semi-cylindrical specimen is presented in Figure 10. Similar to the rectangular specimen, crack initiation originated at the predefined notch and propagated upward toward the asphalt overlay. Although the specimen geometry differed, the overall crack trajectory remained nearly vertical, indicating that the fracture process was governed primarily by the tensile stress field generated beneath the loading point.

Figure 10. Post-test fracture pattern of the semi-cylindrical asphalt-overlaid PCC specimen following three-point bending

Comparison of the two specimen geometries indicates that the crack initiation location and propagation direction were largely independent of specimen shape. In both configurations, fracture developed within the PCC layer before approaching the asphalt overlay, where crack penetration became less pronounced. This behavior suggests that the asphalt layer influenced local stress redistribution near the interface, reducing the crack propagation rate as the fracture approached the overlay. Overall, the experimental observations demonstrate that the proposed laboratory methodology provides a repeatable representation of bottom-up reflective cracking suitable for subsequent distributed strain monitoring and numerical validation. No secondary cracking, crack branching, or interface debonding was observed during the experiments, indicating that fracture propagation was dominated by Mode-I tensile cracking.

4.2 Distributed Strain Localization During Crack Propagation

To quantify fracture development, crack widths were measured at multiple locations along the crack height after completion of each three-point bending test. These measurements provide a quantitative assessment of crack opening and allow the variation of fracture displacement through the specimen thickness to be examined.

The crack-width distribution measured for the rectangular specimen is presented in Figure 11. The largest crack opening occurred immediately above the predefined notch, where the maximum principal tensile stress developed during flexural loading. Crack width decreased progressively with increasing distance from the notch, approaching negligible values near the asphalt overlay. The maximum crack width was approximately 7.55 mm, while the crack opening near the upper portion of the PCC layer decreased to approximately 0.04 mm, corresponding to a reduction of more than 99%.

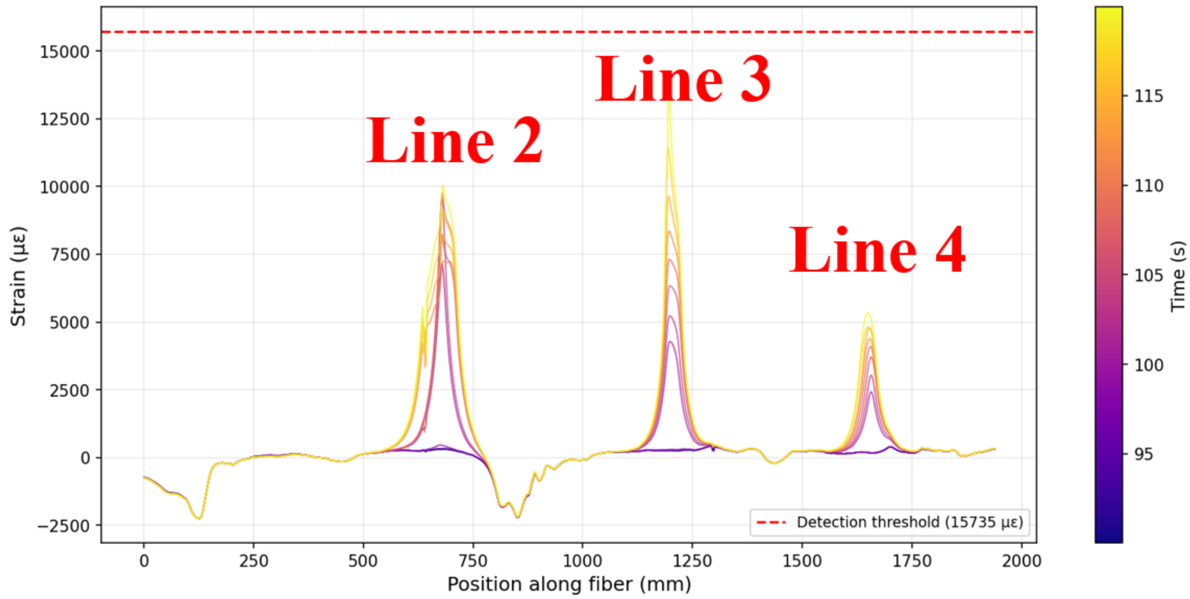

Figure 11. **Evolution of distributed strain along the sensing fiber in the rectangular specimen during three-point bending. Localized strain peaks correspond to sensing Lines 2–4 intersected by the propagating crack.**

The corresponding measurements for the semi-cylindrical specimen are shown in Figure 12. A similar trend was observed, with the maximum crack opening occurring near the notch and decreasing continuously toward the asphalt overlay. However, the maximum crack width reached approximately 11.65 mm, indicating greater localized deformation before complete fracture compared with the rectangular specimen.

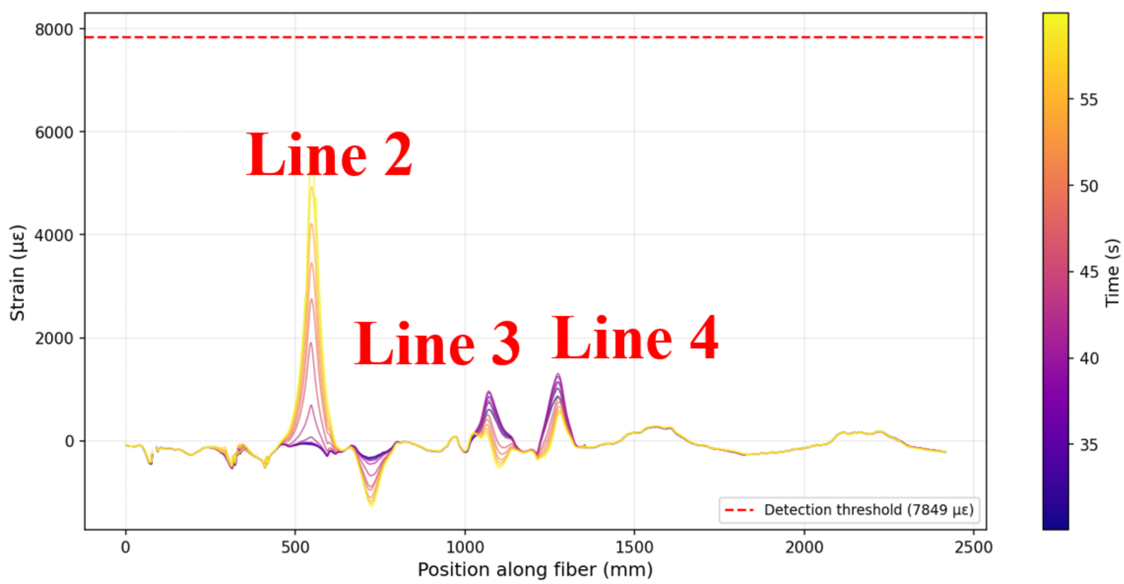

Figure 12. **Evolution of distributed strain along the sensing fiber in the semi-cylindrical specimen during three-point bending. Localized strain peaks indicate crack–fiber intersections along sensing Lines 2–4.**

The measured crack-width distributions are consistent with the flexural stress field generated during three-point bending. According to classical beam theory, tensile stresses reach their maximum value at the bottom surface of the specimen and decrease toward the neutral axis [68]. Consequently, the crack opening displacement is largest near the crack initiation location and progressively decreases as the crack propagates upward through the PCC layer. The smaller crack openings observed near the asphalt overlay further indicate that the stiffness contrast between the PCC and asphalt layers influences local stress redistribution during fracture propagation.

Although the semi-cylindrical specimen exhibited larger crack openings than the rectangular specimen, both geometries demonstrated the same overall fracture mechanism. Crack initiation consistently occurred at the predefined notch, followed by stable upward propagation and progressive reduction in crack opening toward the asphalt overlay. These observations indicate that specimen geometry primarily influences the magnitude of local deformation rather than the fundamental fracture behavior.

4.3 Global Mechanical Response

The global structural response of the pavement specimens was evaluated using the load–displacement curves obtained during the three-point bending tests. The load–displacement relationship provides important information regarding the elastic response, crack initiation, stiffness degradation, and residual load-carrying capacity of the layered pavement system.

The experimental load–displacement responses of the rectangular and semi-cylindrical specimens are compared in Figure 13. Both specimens exhibited an approximately linear response during the initial loading stage, indicating elastic deformation before crack initiation. As loading progressed, the applied load increased until reaching a distinct peak corresponding to crack initiation at the predefined notch. Immediately after the peak load, both specimens experienced a sudden reduction in load, indicating stiffness degradation associated with fracture initiation and propagation.

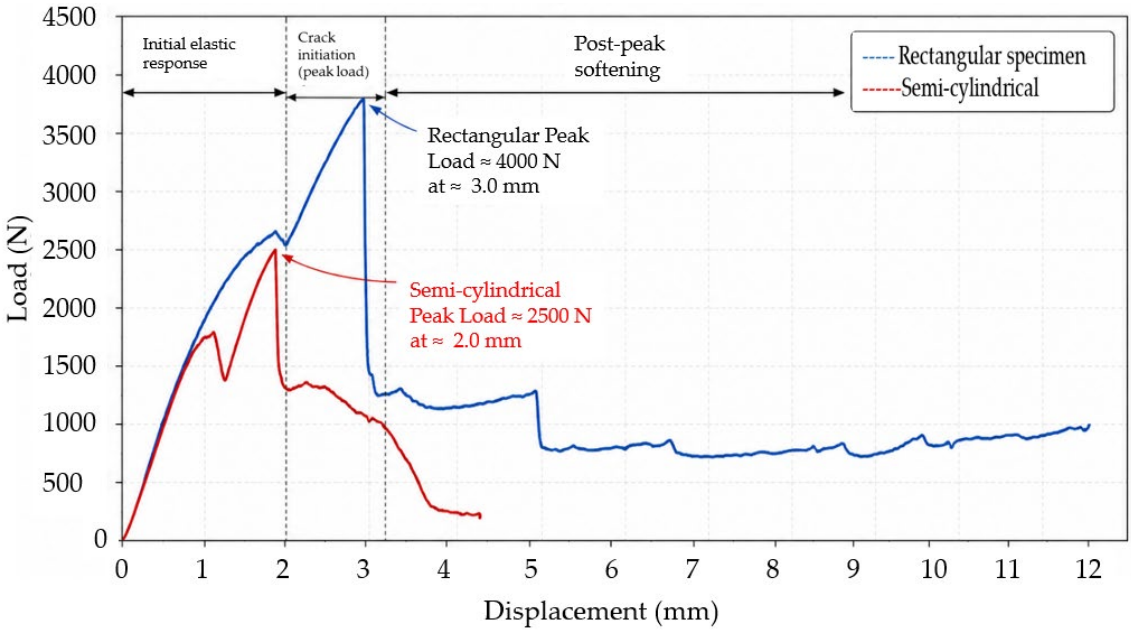

Figure 13. Experimental load–displacement responses of the rectangular and semi-cylindrical specimens subjected to three-point bending

The rectangular specimen reached a higher peak load than the semi-cylindrical specimen and maintained a greater residual load throughout the post-peak region. This behavior indicates a higher load-carrying capacity and greater resistance to fracture under flexural loading. In contrast, the semi-cylindrical specimen exhibited a lower peak load and a more pronounced post-peak load reduction, suggesting more rapid stiffness degradation after crack initiation.

Despite these quantitative differences, both specimens exhibited the same overall sequence of structural response consisting of an initial elastic stage, crack initiation at the predefined notch, rapid post-peak stiffness degradation, and progressive fracture propagation. The load–displacement responses therefore complement the crack observations presented in Sections 4.1 and 4.2, providing a global measure of the mechanical behavior of the layered pavement system.

The global mechanical response presented in this section establishes the basis for interpreting the distributed strain measurements obtained using the OFDR-based DFOS system. While the load–displacement curves characterize the overall structural behavior of the specimens, they do not provide information regarding the spatial evolution of localized deformation preceding visible cracking. This limitation is addressed in the following section through distributed strain measurements, which enable crack initiation and propagation to be monitored continuously along the sensing fiber.

4.4 DFOS Monitoring Results

The OFDR-based DFOS system enabled continuous monitoring of localized deformation throughout the three-point bending tests. Unlike conventional strain gauges, which provide measurements only at discrete locations, the distributed optical fiber functions as a continuous sensing element, allowing strain variations to be monitored along the entire sensing length. This distributed sensing capability makes DFOS particularly suitable for investigating bottom-up reflective cracking, where the exact crack initiation and propagation path cannot be determined a priori.

Following completion of the mechanical tests, the specimens were examined to evaluate the relationship between the final crack path and the installed sensing fibers. Figure 14 presents the post-test rectangular specimen after removal from the testing frame. The figure illustrates the surface-bonded DFOS sensing fibers, the predefined notch, and the final crack propagation path produced during three-point bending. Crack initiation occurred at the predefined notch located at the bottom of the PCC layer and propagated vertically upward toward the asphalt overlay, intersecting multiple sensing fibers during its progression.

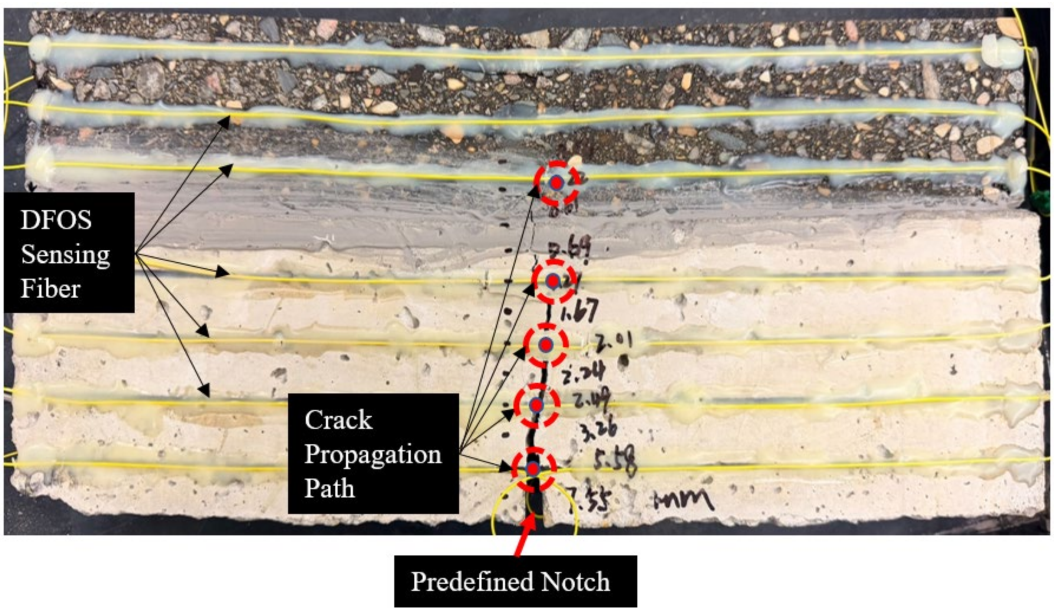

Figure 14. Annotated post-test photograph of the rectangular asphalt-overlaid PCC specimen showing the surface-bonded DFOS sensing fibers, predefined notch, and bottom-up crack propagation path following three-point bending

The crack intersected several parallel sensing paths as it propagated through the specimen thickness. Because the optical fiber continuously measured strain along its entire length, each intersection between the crack path and a sensing fiber corresponded to a localized strain concentration during loading. Consequently, the distributed sensing network captured the evolution of crack propagation at multiple elevations rather than at a single measurement location. This demonstrates one of the principal advantages of distributed fiber optic sensing over conventional point-based instrumentation, where damage occurring between sensors may remain undetected.

The selected serpentine sensing layout proved effective for monitoring bottom-up crack development. The approximately 20-mm spacing between adjacent sensing paths provided sufficient spatial coverage to ensure that the propagating crack intersected multiple fiber segments as it advanced through the PCC layer. As a result, strain localization associated with crack initiation and subsequent crack growth could be identified continuously throughout the loading process. The successful interaction between the crack path and the sensing network confirms that the sensing layout developed in Section 3.3 is appropriate for monitoring reflective cracking in layered pavement systems.

A similar sensing response was observed for the semi-cylindrical specimen, as shown in Figure 15. Despite the difference in specimen geometry, the crack again initiated at the predefined notch and propagated upward through the PCC layer while intersecting multiple sensing paths. The distributed fiber layout therefore remained effective under both specimen configurations, demonstrating that the proposed monitoring strategy is robust and does not depend on specimen geometry.

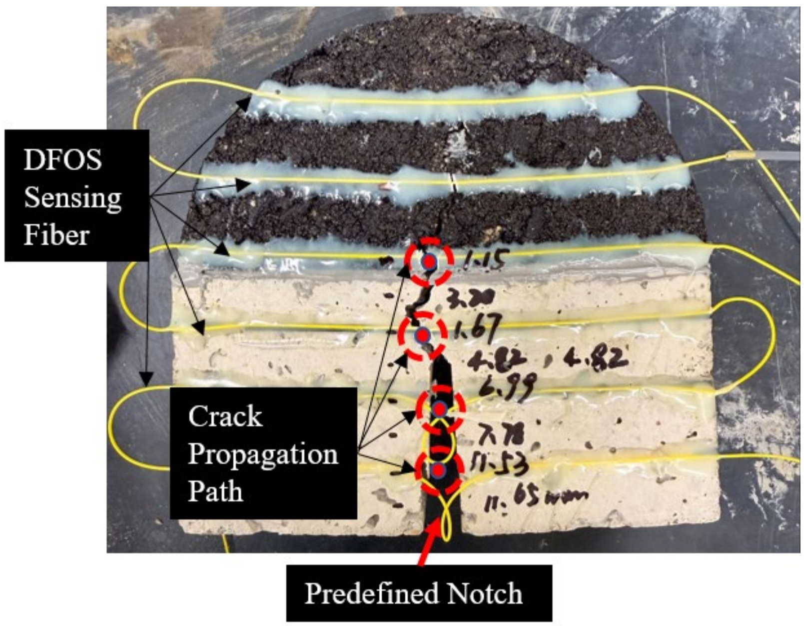

Figure 15. Annotated post-test photograph of the semi-cylindrical asphalt-overlaid PCC specimen showing the DFOS sensing fiber layout and bottom-up crack propagation following three-point bending

Although the post-test photographs identify the final crack trajectory, the primary contribution of the OFDR-based DFOS system lies in its ability to monitor strain evolution continuously throughout the loading process. Localized strain concentrations developed at the sensing paths intersected by the propagating crack, enabling damage to be detected before complete crack penetration became visually apparent. This capability provides significant advantages for SHM applications, where early identification of localized damage is essential for condition assessment and maintenance planning.

The distributed sensing observations presented in this section establish the experimental basis for interpreting the finite element simulations presented in the following section. In particular, the experimentally observed crack trajectory and sensing locations are compared with the numerically predicted stress concentrations to evaluate the capability of the proposed hybrid experimental–numerical framework to characterize bottom-up reflective cracking in rehabilitated pavement systems.

4.5 Finite Element Analysis of Crack Initiation and Propagation

Finite element simulations were conducted to investigate the internal stress redistribution governing bottom-up reflective cracking in the layered pavement specimens. While the laboratory experiments provided direct observations of crack development and the DFOS system monitored localized deformation during loading, the numerical model enabled visualization of the internal stress field responsible for crack initiation and subsequent propagation. The simulations therefore provide a mechanistic interpretation of the fracture process that cannot be obtained through experimental observations alone.

The evolution of the predicted stress field for both the rectangular and semi-cylindrical specimens is presented in Figure 16 and 17. The numerical results demonstrate a progressive transition from localized stress concentration at the predefined notch to upward crack propagation through the PCC layer as the applied displacement increased. Despite the different specimen geometries, both configurations exhibited similar stress redistribution patterns throughout the loading process.

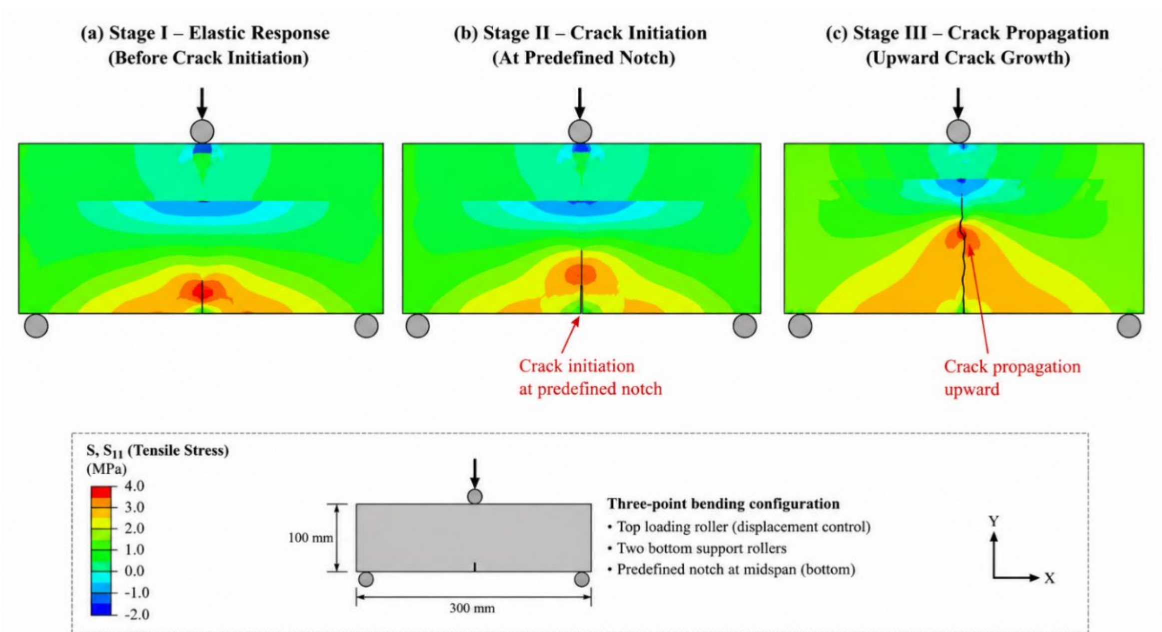

Figure 16. Evolution of the tensile stress field predicted by the ABAQUS finite element model for the rectangular asphalt-overlaid PCC specimen during three-point bending. The three loading stages illustrate (a) elastic response, (b) crack initiation at the predefined notch, and (c) upward crack propagation accompanied by stress redistribution.

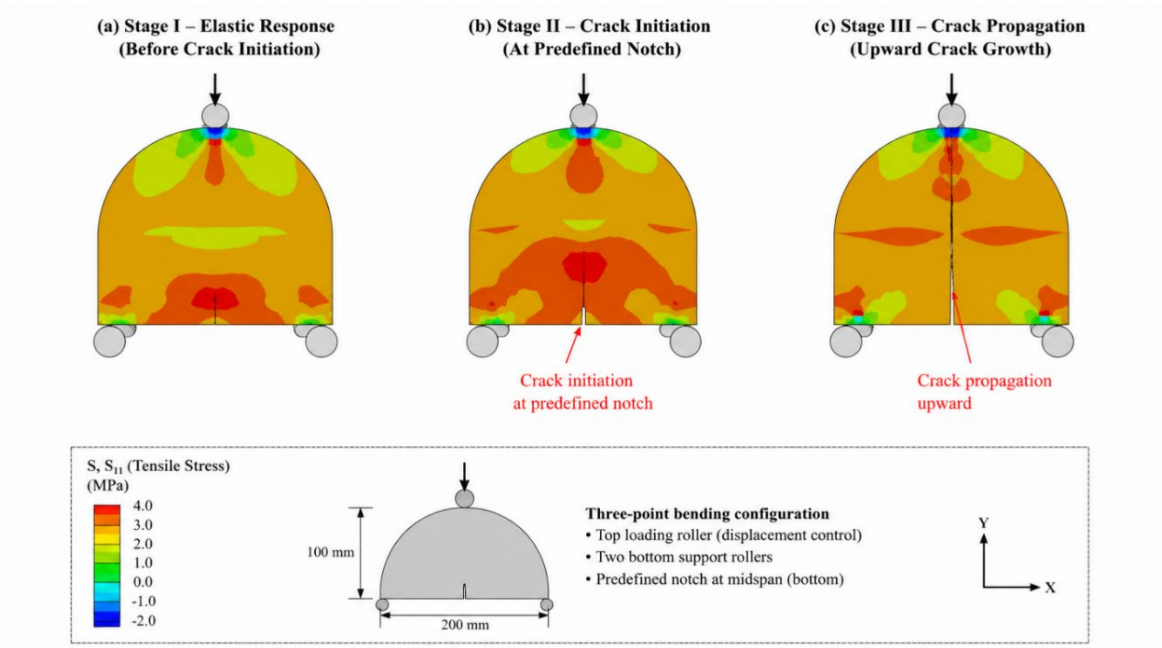

Figure 17. Evolution of the tensile stress field predicted by the ABAQUS finite element model for the semi-cylindrical pavement specimen during three-point bending.

During the initial loading stage, tensile stresses were distributed relatively uniformly throughout the lower portion of the PCC layer, with the highest stresses developing directly above the predefined notch. Because the notch introduces a geometric discontinuity, it acts as a stress concentrator that significantly increases the local tensile stress. Consequently, crack initiation consistently occurred at this location, in agreement with the fracture patterns observed experimentally.

As the applied displacement increased, the magnitude of the tensile stress surrounding the notch increased rapidly, producing localized stress concentration at the crack tip. Once crack initiation occurred, the stress field was redistributed around the advancing fracture front, resulting in progressive upward crack propagation. Rather than remaining concentrated at the original notch location, the region of maximum tensile stress migrated with the crack tip, demonstrating the characteristic stress redistribution associated with quasi-brittle fracture under flexural loading.

The simulations further indicate that crack propagation was governed primarily by Mode-I tensile fracture. The predicted crack trajectory remained nearly vertical throughout the PCC layer, with minimal lateral deviation, indicating that tensile stresses dominated the fracture process under the symmetric three-point bending configuration. This numerical behavior closely resembles the experimentally observed crack paths presented in Section 4.1, confirming that the adopted loading configuration successfully reproduced the bottom-up reflective cracking mechanism.

Although both specimen geometries exhibited similar fracture mechanisms, differences were observed in the spatial distribution of the stress field. The rectangular specimen developed a relatively narrow stress concentration zone that remained localized around the advancing crack tip. In contrast, the semi-cylindrical specimen exhibited a broader region of elevated tensile stress, indicating more gradual stress redistribution within the curved geometry. This behavior is consistent with the larger crack openings measured experimentally in the semi-cylindrical specimens and suggests that specimen geometry influences the extent of local deformation while having only a limited effect on the overall crack propagation mechanism.

As the fracture progressed toward the asphalt overlay, the numerical simulations predicted a gradual redistribution of tensile stresses across the asphalt–PCC interface. The stiffness contrast between the two pavement layers reduced the stress concentration intensity as the crack approached the interface, thereby limiting the fracture's complete penetration into the asphalt overlay. This prediction agrees with the experimental observations, in which crack development was primarily confined to the PCC layer, with only limited propagation observed within the asphalt overlay.

Overall, the finite element model successfully reproduced the principal stages of bottom-up reflective cracking observed during laboratory testing, including tensile stress localization above the predefined notch, crack initiation, progressive upward fracture propagation, and crack-tip stress redistribution. The close correspondence between the simulated fracture behavior and the experimental observations demonstrates that the numerical model provides a reliable representation of the dominant fracture mechanisms governing reflective cracking in asphalt-overlaid PCC pavements. These numerical predictions establish the basis for the comprehensive experimental–numerical validation presented in the following section.

4.6 Experimental–Numerical Validation

The reliability of the proposed hybrid experimental–numerical framework was evaluated by comparing finite element predictions with laboratory observations and DFOS measurements. Rather than relying on a single validation criterion, the proposed methodology integrates multiple independent datasets, including crack initiation location, crack propagation path, global load–displacement response, and distributed strain monitoring. Agreement among these complementary observations provides confidence that the proposed framework accurately captures the mechanisms governing bottom-up reflective cracking in asphalt-overlaid PCC pavements. Figure 18 summarizes the comparison between the numerical simulations and the experimental observations for both the rectangular and semi-cylindrical specimens. The figure combines the evolution of the simulated tensile stress field, the experimentally observed crack development, and the corresponding global load–displacement responses obtained during three-point bending. The close correspondence between these independent datasets demonstrates the consistency of the proposed methodology across different specimen geometries.

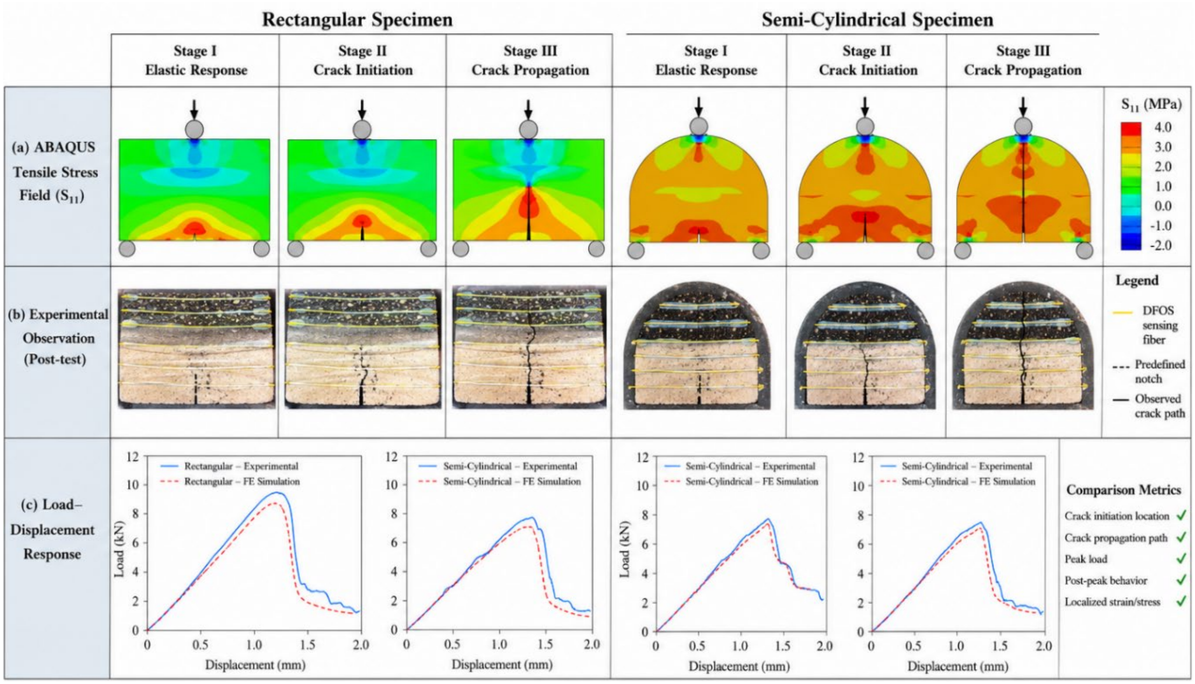

Figure 18. Experimental–numerical validation of bottom-up reflective cracking in rectangular and semi-cylindrical pavement specimens. The figure compares (a) finite element tensile stress evolution, (b) experimentally observed crack propagation, and (c) global load–displacement responses obtained during three-point bending.

The first level of validation considered the crack initiation location. In both specimen configurations, the FEM predicted the highest tensile stresses immediately above the predefined notch during the early stages of loading. Experimentally, crack initiation consistently occurred at the same location, confirming that the numerical model accurately identified the critical tensile region responsible for fracture initiation. This agreement verifies that the specimen geometry, loading configuration, and material representation adopted in the numerical model successfully reproduce the onset of bottom-up reflective cracking.

The second level of validation focused on crack propagation. The numerical simulations predicted a predominantly vertical crack trajectory extending upward through the PCC layer toward the asphalt overlay. Similar crack paths were observed experimentally in both specimen geometries, with only minor deviations from the specimen centerline. Furthermore, the numerical results captured the progressive upward migration of the fracture front and the associated redistribution of tensile stresses around the crack tip. The close correspondence between the predicted and observed crack trajectories demonstrates that the finite element model accurately represents the dominant fracture mechanism under three-point bending.

The third level of validation examined the global structural response. The experimentally measured load–displacement curves exhibited an initial linear-elastic region, followed by a peak load corresponding to crack initiation, and a subsequent reduction in load-carrying capacity associated with fracture propagation. The finite element simulations reproduced the same sequence of structural behavior, including the initial stiffness, peak response, and post-peak softening. Although minor differences were observed after crack initiation, the overall agreement indicates that the numerical model successfully captures the global mechanical response of the layered pavement specimens.

The distributed fiber-optic sensing observations provide an additional level of validation by linking the experimentally observed crack development to the predicted stress field. As discussed in Section 4.4, the propagating crack intersected five distributed sensing paths, producing localized strain concentrations along the sensing network. The locations of experimentally observed crack propagation closely match the regions of maximum principal tensile stress predicted by the finite element simulations, demonstrating that the distributed sensing system effectively identifies the same critical regions as the numerical model. This agreement confirms that the selected serpentine sensing layout provides sufficient spatial coverage for monitoring bottom-up reflective cracking.

Comparison of the rectangular and semi-cylindrical specimens further demonstrates the robustness of the proposed framework. Although the two geometries exhibited differences in local stress distributions and crack-opening magnitudes, both experimental and numerical investigations consistently identified the same fracture mechanism. In each case, crack initiation occurred at the predefined notch, propagated predominantly in the vertical direction, and remained largely confined to the PCC layer before approaching the asphalt overlay. These consistent observations indicate that the proposed hybrid framework is applicable across different specimen geometries and provide reliable characterization of bottom-up reflective cracking.

The principal findings of the experimental–numerical validation are summarized in Table 6. The comparison demonstrates strong agreement between the laboratory observations and the finite element predictions across all major validation criteria, including crack initiation, crack propagation, global structural response, and DFOS-based monitoring. Collectively, these results confirm that the proposed framework successfully captures both the global mechanical behavior and the localized fracture mechanisms associated with bottom-up reflective cracking.

Table 6. Summary of the experimental–numerical validation results

Validation criterion	Experimental observation	Numerical prediction	Validation outcome
Crack initiation	Crack originated at predefined notch	Maximum principal tensile stress developed at notch	Excellent agreement
Crack propagation	Vertical crack growth through PCC	Similar crack trajectory	Excellent agreement
Crack confinement	Crack largely confined to PCC layer	Damage localized within PCC layer	Good agreement
Load–displacement response	Elastic response followed by peak load and post-peak softening	Similar global response	Good agreement
DFOS monitoring	Crack intersected multiple sensing fibers	Stress localization coincided with crack path	Excellent agreement

The proposed hybrid monitoring framework provides a practical methodology for evaluating rehabilitation strategies before field implementation. By continuously monitoring strain localization and relating it to internal stress redistribution, the framework can assist pavement engineers in optimizing overlay thickness, rehabilitation materials, and maintenance scheduling. Furthermore, the demonstrated capability of OFDR-based DFOS suggests considerable potential for future full-scale structural health monitoring of transportation infrastructure.

5. SUMMARY

This study presented a hybrid experimental–numerical framework for investigating bottom-up reflective cracking in rehabilitated asphalt-overlaid PCC pavements. The proposed methodology integrates laboratory-scale three-point bending experiments, OFDR-based DFOS, and finite-element (ABAQUS) simulations to investigate crack initiation, propagation, stress redistribution, and strain localization in layered pavement systems. By combining experimental observations with numerical analysis, the framework provides a comprehensive understanding of the fracture mechanisms governing bottom-up reflective cracking.

The laboratory experiments successfully reproduced the characteristic bottom-up cracking mechanism observed in rehabilitated pavements. In both the rectangular and semi-cylindrical specimens, cracks consistently initiated at the predefined notch within the PCC layer and propagated vertically toward the asphalt overlay under three-point bending. Crack-width measurements further confirmed that the largest crack openings occurred near the crack initiation region and progressively decreased toward the asphalt overlay, consistent with the expected flexural stress distribution.

The OFDR-based DFOS system successfully monitored the evolution of localized deformation throughout the loading process. The distributed sensing layout provided continuous strain measurements over the monitored region and demonstrated the capability to identify localized deformation associated with crack initiation and propagation. Unlike conventional point sensors, the distributed sensing approach enabled full-field monitoring without requiring prior knowledge of the crack location, highlighting its potential for early damage detection and structural health monitoring of layered pavement systems.

The finite element simulations provided a physics-based interpretation of the experimentally observed fracture behavior by capturing the evolution of tensile stress concentrations, crack initiation, and progressive stress redistribution during loading. The predicted crack initiation location, crack trajectory, and global structural response showed good agreement with the laboratory observations. Furthermore, the experimental–numerical validation demonstrated consistent agreement among the crack patterns, load–displacement responses, DFOS observations, and finite element predictions, confirming the reliability of the proposed framework for characterizing bottom-up reflective cracking.

Overall, this research demonstrates that integrating distributed fiber optic sensing with finite element analysis provides a robust methodology for studying fracture processes in rehabilitated pavement systems. The proposed framework enables continuous monitoring of crack development while simultaneously providing a mechanistic interpretation of the underlying stress redistribution. These capabilities offer significant potential for SHM, condition assessment, and rehabilitation planning of transportation infrastructure, where early identification of reflective cracking can support more effective maintenance strategies and extend pavement service life.

Although the proposed framework successfully characterizes bottom-up reflective cracking under controlled laboratory conditions, several limitations should be acknowledged. The experiments were conducted on laboratory-scale specimens subjected to monotonic loading under constant environmental conditions. Consequently, the influence of cyclic traffic loading, temperature fluctuations, moisture effects, and long-term material aging were not considered. Furthermore, the numerical model assumes idealized material behavior and a perfectly bonded asphalt–PCC interface, which may differ from field conditions. These limitations should be considered when extending the proposed methodology to full-scale pavement systems.

5.1 Major Contributions of this Study:

- Developed a hybrid experimental–numerical framework integrating laboratory testing, OFDR-based DFOS, and finite element modeling for investigating bottom-up reflective cracking.
- Demonstrated that OFDR-based distributed sensing can continuously monitor strain localization preceding visible crack formation.
- Experimentally quantified crack initiation, propagation, and crack-width evolution in rehabilitated asphalt-overlaid PCC pavement specimens.
- Established strong agreement among experimental observations, distributed strain measurements, and finite element predictions.
- Demonstrated the potential of distributed fiber optic sensing for structural health monitoring and early damage detection in rehabilitated pavement systems.

6. FUTURE RESEARCH

While the proposed hybrid experimental–numerical framework successfully characterized bottom-up reflective cracking under controlled laboratory conditions, several opportunities remain to extend its capability toward field-scale, long-term monitoring of rehabilitated concrete pavements. Future research is recommended along the following directions.

6.1 Cyclic and Fatigue Loading

The present investigation applied monotonic three-point bending to induce controlled crack initiation and propagation. Future studies should extend the framework to repeated and cyclic loading representative of actual traffic in order to capture fatigue-driven reflective crack growth, crack propagation rates, and the accumulation of damage over many load repetitions. Wheel-tracking devices and accelerated pavement testing would allow the DFOS-monitored fatigue response to be linked to field performance and remaining service life.

6.2 Coupled Thermal and Environmental Effects

All experiments were conducted under constant laboratory conditions, so temperature fluctuations, moisture, and freeze–thaw cycling were not considered. Because thermally induced joint movement is a primary driver of reflective cracking—particularly in cold regions such as North Dakota—future work should incorporate thermal cycling and coupled thermo-mechanical loading, together with temperature-compensated distributed sensing, to separate mechanical strain from thermal strain and quantify the environmental contribution to crack development.

6.3 Interface Behavior and Slab-fracturing Treatments

The finite element model assumed a perfectly bonded asphalt–PCC interface. Future models should represent partial bonding and progressive interfacial debonding using cohesive-zone or contact-based interface formulations, and the experimental program should incorporate specimens prepared with representative slab-fracturing treatments (crack-and-seat, break-and-seat, and rubblization) to evaluate how each treatment alters stress redistribution and reflective crack propagation.

6.4 Machine learning–assisted interpretation

The high spatial density of OFDR measurements produces large datasets whose interpretation is currently performed manually. Future research should develop machine learning and data-driven models to automatically detect crack initiation, localize damage, and estimate crack width from distributed strain signatures, supporting real-time condition assessment and eventual integration into a digital-twin representation of the pavement.

7. REFERENCES

1. Acharya, A. and T. Kogure, "Application of novel distributed fiber-optic sensing for slope deformation monitoring: a comprehensive review." *International Journal of Environmental Science and Technology*, 2023. 20(7): p. 8217-8240.
2. Mahmood, Y., et al., "Embedded GFRP-packaged sensor system for real-time and high-precision vehicle load estimation in weigh-in-motion (WIM) applications." *Measurement Science and Technology*, 2026. 37(9).
3. Aung, T., et al., "Advanced Structural Health Monitoring Method by Integrated Isogeometric Analysis and Distributed Fiber Optic Sensing." *Sensors*, 2021. 21(17).
4. Baek, J., I. Al-Qadi, and TRB, "Finite element method modeling of reflective cracking initiation and propagation - Investigation of the effect of steel reinforcement interlayer on retarding reflective cracking in hot-mix asphalt overlay," in *Pavement Rehabilitation, Strength and Deformation Characteristics, and Surface Properties-Vehicle Interaction* 2006. 2006. p. 32–42.
5. Alshandah, M., et al., "Internal crack detection in concrete pavement using discrete strain sensors." *Journal of Civil Structural Health Monitoring*, 2020. 10(2): p. 345–356.
6. Beheshti, M. and H. Ozer, "Viscoelastic Computational Fracture Mechanics Approach for the Analysis of Thermal Reflective Cracking in Asphalt Overlaid Jointed Concrete Airfield Pavements." *Transportation Research Record*, 2025. 2679(12): p. 823–843.
7. Badin, G., et al., "Evaluation of Pigment-Modified Clear Binders and Asphalts: An Approach towards Sustainable, Heat Harvesting, and Non-Black Pavements." *Infrastructures*, 2024. - 9(- 5).
8. Riaz, A., et al., "Innovative Pavement Solutions: A Comprehensive Review from Conventional Asphalt to Sustainable Colored Alternatives." *Infrastructures* 2024. 9(10): p. 35.
9. Dave, E. and W. Buttlar, "Thermal reflective cracking of asphalt concrete overlays." *International Journal of Pavement Engineering*, 2010. 11(6): p. 477–488.
10. Fischer, O., S. Thoma, and S. Crepaz, "Distributed fiber optic sensing for crack detection in concrete structures." *Civil Engineering Design*, 2019; 1: 97–105.11. Deng, Y., et al., "Determination of flexible pavement deterioration conditions using Long-Term Pavement Performance database and artificial intelligence-based finite element model updating." *Structural Control & Health Monitoring*, 2021. 28(2).
12. Kindler, A., et al., "Long-term crack monitoring of prestressed concrete structures by means of distributed fiber-optic strain sensing." *Bautechnik*, 2023. 100(7): p. 383–395.
13. Diallo, A. and M. Akpinar, "Mechanistic Responses of Asphalt Concrete Overlay over Jointed Plain Concrete Pavement using Finite Element Method." *Baltic Journal of Road and Bridge Engineering*, 2020. 15(5): p. 80–93.
14. Liao, X., et al., "Deep convolutional transformer network for quantifying crack width in tunnel lining structures using distributed fiber optic sensing data." *Smart Materials and Structures*, 2025. 34(3).

15. Jiao, L., R. Wu, and J. Harvey, “Reflective crack initiation of asphalt overlays on jointed concrete pavement using finite element model.” *International Journal of Pavement Engineering*, 2023. 24(2).

16. Ou, R., L. Luo, and K. Soga, “Distributed fiber optic strain sensing for crack detection with Brillouin shift spectrum back analysis.” *Structural Health Monitoring-An International Journal*, 2024. 23(4).

17. Richter, B., M. Herbers, and S. Marx, “Crack monitoring on concrete structures with distributed fiber optic sensors-Toward automated data evaluation and assessment.” *Structural Concrete*, 2024. 25(2): p. 1465–1480.

18. Bednarz, B. et al., “Distributed Fiber Optic Sensing (DFOS) for Deformation Assessment of Composite Collectors and Pipelines.” *Sensors*, 2021. 21(17).

19. Shestakov, A., et al., “Implementation of a Length Gauge Based on Optical Frequency Domain Reflectometry (OFDR).” *Sensors*, 2026. 26(2).

20. Ding, Z., et al., “Distributed Optical Fiber Sensors Based on Optical Frequency Domain Reflectometry: A review.” *Sensors*, 2018. 18(4).

21. Zhang, X., et al., “Smart sensing of concrete crack using distributed fiber optics sensors: Current advances and perspectives.” *Case Studies in Construction Materials*, 2025. 22.

22. Karadag, H., et al., “Determination of permanent deformation of flexible pavements using finite element model.” *Gradevinar*, 2022. 74(6): p. 471–480.

23. Karapanagiotis, C., K. Hicke, and K. Krebber, “A collection of machine learning assisted distributed fiber optic sensors for infrastructure monitoring.” *tm - Technisches Messen*, 2023. 90(3): p. 177–195.

24. Khazanovich, L., et al., “Investigation and Modification of Available Mechanistic-Empirical Procedures for Reflective Cracking in Asphalt Overlays of Concrete Pavements.” *Transportation Research Record*, 2013(2368): p. 126–132.

25. Kim, H. and W. Buttlar, “Finite element cohesive fracture modeling of airport pavements at low temperatures.” *Cold Regions Science and Technology*, 2009. 57(2-3): p. 123–130.

26. Kobayashi, M., et al., “Shape sensing for CFRP and aluminum honeycomb sandwich panel using inverse finite element method with distributed fiber-optic sensors.” *Composite Structures*, 2023. 308.

27. Lei, X., Z. Xue, and T. Hashimoto, “Fiber Optic Sensing for Geomechanical Monitoring: (2)- Distributed Strain Measurements at a Pumping Test and Geomechanical Modeling of Deformation of Reservoir Rocks.” *Applied Sciences-Basel*, 2019. 9(3).

28. Hernandez, J., V. Bevan, and S. Underwood, “Three-dimensional finite element modelling of rigid pavement buckling.” *International Journal of Pavement Engineering*, 2026. 27(1).

29. Kumar, Y., A. Trivedi, and S. Shukla, “Damage Evaluation in Pavement-Geomaterial System Using Finite Element-Scaled Accelerated Pavement Testing.” *Transportation Infrastructure Geotechnology*, 2024. 11(3): p. 922–933.

30. Ziari, H., M. Keymanesh, and M. Khabiri, “Finite-element modelling of crack sealant flexible pavement.” *Baltic Journal of Road and Bridge Engineering*, 2007. 2(2): p. 89–93.

31. Mahmood, Y., et al., "Fiber-Optic Sensor-Based Structural Health Monitoring with Machine Learning: A Task-Oriented and Cross-Domain Review." *Sensors*, 2026. 26(9).

32. Yin, W., et al., "Damage identification of CFRP laminate based on finite element analysis and FBG sensor network." *Optical Fiber Technology*, 2022. 73.

33. Liu, H., et al., "Distributed fiber-optic sensing of reinforced concrete arch ribs to monitor plastic hinge formation." *Structural Health Monitoring-an International Journal*, 2025.

34. Liu, J., et al., "Urban Monitoring Using Preexisting Telecommunication Fiber-Optic Networks for Distributed Acoustic Sensing: A Review." *IEEE Sensors Journal*, 2025. 25(21): p. 39353–39370.

35. Gu, F., et al., "Influences of slab fracturing techniques on long-term performance of rehabilitated PCC pavements." *International Journal of Pavement Engineering*, 2022. 23(5): p. 1422–1432.

36. Beheshti, M., et al., "Analysis of reflective cracking in asphalt overlaid jointed concrete airfield pavements using a 3D generalized finite element approach*." International Journal of Pavement Engineering*, 2024. 25(1).

37. Irfan, M., et al., "Highway Asset Management Framework for Longevity of Infrastructure – A Case Study for China-Pakistan Economic Corridor." *American Journal of Civil Engineering*, 2019. 6(6): p. 185–194.

38. Hou, F., et al., "Research on the Anti-Reflective Cracking Performance of a Full-Depth Asphalt Pavement." *Sustainability*, 2021. 13(17).

39. Mehmood, Y., H. Zahoor, and F. Ullah, "Economic-Efficiency Analysis of Rawalpindi Bypass Project: A Case Study." *Innovative Production and Construction*, 2018. 2: p. 531–555.

40. Liu, F., et al., "Asphalt concrete overlay thermal reflective cracking stress intensity factor prediction using machine learning." *Road Materials and Pavement Design*, 2025.

41. Rema, A. and A. Swamy, "Response Surface-Based Approach to Quantify Variability in Recycled-Asphalt Concrete Mixtures." *Journal of Materials in Civil Engineering*, 2022. 34(11).

42. Kumar, P. and M. Sharma, "Modified pavement condition assessment model for asphalt concrete pavements." *International Journal of System Assurance Engineering and Management*, 2024. 15(3): p. 839–853.

43. Vyas, V., A. Singh, and A. Srivastava, "Entropy-based fuzzy SWOT decision-making for condition assessment of airfield pavements." *International Journal of Pavement Engineering*, 2021. 22(10): p. 1226–1237.

44. You, L., et al., "Influence of anisotropy on structural dynamic response, from the views of mechanism, analysis method, and implications for pavement design." *International Journal of Pavement Engineering*, 2025. 26(1).

45. El Hakea, A. and M. Fakhr, "Recent computer vision applications for pavement distress and condition assessment." *Automation in Construction*, 2023. 146.

46. Altabey, W., "A framework based on deep learning and the intelligent sensors for pavement assessment condition." *Sound and Vibration*, 2025. 59(6).

47. Gajurel, A., et al., “Application of Satellite-Based Remote Sensing for the Management of Pavement Infrastructure Assets.” *Transportation Research Record*, 2024. 2678(9): p. 623–638.

48. Ni, F., et al., “Long-Term Pavement Performance of Quiet Friction Course in Florida.” *Transportation Research Record*, 2026.

49. Zhou, Y., et al., “Measuring asphalt pavement surface texture using a multi-view stereo-based approach.” *International Journal of Pavement Engineering*, 2025. 26(1).

50. Hubbard, P., et al., “Road deformation monitoring and event detection using asphalt-embedded distributed acoustic sensing (DAS).” *Structural Control & Health Monitoring*, 2022. 29(11).

51. Wu, T., et al., “Research Status and Development Trend of Piezoelectric Accelerometer.” *Crystals*, 2023. 13(9).

52. Eichner, D., M. Giousouf, and W. von Münch, “Measurements on micromachined silicon accelerometers with piezoelectric sensor action.” *Sensors and Actuators A-Physical*, 1999. 76(1-3): p. 247–252.

53. Hauswirth, D., et al., “Measuring strain distributions in an asphalt pavement using fibre optic sensors under static loading by test vehicles.” *Road Materials and Pavement Design*, 2025. 26(5): p. 1023–1040.

54. Fuhr, P. and D. Huston, “Corrosion detection in reinforced concrete roadways and bridges via embedded fiber optic sensors.” *Smart Materials & Structures*, 1998. 7(2): p. 217–228.

55. Tian, P., et al., “Optimization Analysis for Pavement Construction Integrated Optical Fiber Sensors Based on DEM-FDM Coupled Method.” *Materials*, 2026. 19(6).

56. Shi, B., et al., “DFOS Applications to Geo-Engineering Monitoring.” *Photonic Sensors*, 2021. 11(2): p. 158–186.

57. Han, G., et al., “Integrated Silicon Photonics OFDR System for High-Resolution Distributed Measurements Based on Rayleigh Backscattering.” *Journal of Lightwave Technology*, 2024. 42(9): p. 3482–3493.

58. Felicita, M., et al., “Assessment of in-situ stress distribution and mechanical properties of wooden foundation piles instrumented with distributed fiber optic sensors (DFOS).” *Case Studies in Construction Materials*, 2024. 20.

59. Ramakrishnan, A. and I. Al-Qadi, “Validated Finite-Element Model for Predicting Asphalt Concrete Overlay Reflective Cracking Potential.” *Transportation Research Record*, 2024. 2678(11): p. 1409–1422.

60. Garzon, J., C. Duarte, and W. Buttlar, “Analysis of Reflective Cracks in Airfield Pavements using a 3-D Generalized Finite Element Method.” *Road Materials and Pavement Design*, 2010. 11(2): p. 459–477.

61. Zhang, J., et al., “Reflective Crack Propagation and Control in Asphalt Pavement Widening.” *Journal of Testing and Evaluation*, 2016. 44(2): p. 838–846.

62. Wang, X. and Y. Zhong, “Influence of tack coat on reflective cracking propagation in semi-rigid base asphalt pavement.” *Engineering Fracture Mechanics*, 2019. 213: p. 172–181.

63. Xie, P. and H. Wang, “Finite element analysis of thermal-induced reflective cracking in composite pavement with mitigation strategies.” *Engineering Fracture Mechanics*, 2022. 266.

64. Rith, M. and S. Lee, “Development of cohesive-zone-based prediction model for reflective cracking in asphalt overlay.” *International Journal of Pavement Engineering*, 2022. 23(4): p. 1050–1059.

65. Saw, J., et al., “Distributed Fiber Optic Sensing for in-well hydraulic fracture monitoring.” *Geoenergy Science and Engineering*, 2025. 250.

66. Siahkouhi, M., et al., “AI-assisted fibre optic sensing frameworks for automated monitoring of railway infrastructure.” *Journal of Infrastructure Intelligence and Resilience*, 2026. 5(2).

67. Shayesteh, A., et al., “Finite Element Method in Statistical Analysis of Flexible Pavement.” *Journal of Marine Science and Technology-Taiwan*, 2017. 25(2): p. 142–152.

68. Ebrahimi, F. and R. Selvamani, *Mechanics of Smart Magneto-electro-elastic Nanostructures*, 2021: p. 50.

CTIPS Center for Transformative Infrastructure Preservation and Sustainability

USDOT Region 8 University Transportation Center

NDSU Dept 2880 • P.O. Box 6050
Fargo, ND 58108-6050

(701)231-7767

ndsu.ugpti@ndsu.edu